Transactions of the 14th International Conference on Structural Mechanics in Reactor Technology (SMiRT 14), Lyon, France, August 17-22, 1997 K14/2

An aseismic design of equipment submerged in a pool on a base-isolated building

Shin T.M.
Korea Atomic Energy Research Institute, Korea

ABSTRACT

For submerged internal equipment like spent fuel storage racks in the nuclear power plant, building base-isolation may cause an adverse effect on the seismic response of the equipment exceptionally. Through a seismic analysis of simplified internal equipment model in a base-isolated building, it is discussed about the potential increase of response in extreme case. As design methods to minimize the increased response in this case, an optimization of fluid gap size for the control of hydrodynamic effect and base isolation of the submerged equipment are introduced.

1. INTRODUCTION

Base-isolation of a building (or primary structure) has shown a remarkable performance in seismic response attenuation of its internal (or secondary) equipment through many studies[1,2]. The internal equipment concerned about in the case are mostly in air condition. However, there are some equipment like spent fuel storage racks in nuclear power plant which have to be operated under the submerged condition, and thus experience hydrodynamic resistances against excitations by earthquake[3]. It is known that the fluid coupling between a body and a rigid wall reduces both natural frequencies and modal participation factors of the body compared with the case when they are in air[4]. Noting that most of the base isolation devices generally reduce the fundamental frequency of the building structure, it is easy to expect that building base isolation may have adverse effects by bringing about resonance upon submerged internal equipment.

This paper illustrates such a case through dynamic analyses of a simplified model of submerged internal equipment in a base-isolated building. To reduce the increased response in the case, an optimization of fluid gap size for the control of hydrodynamic effect is attempted. As an alternative for the case that gap control is limited, in addition, a concept of base isolation of the submerged equipment in a base-isolated building is introduced .

2. DYNAMIC MODELING

2.1 Coupled System Model Considering Hydrodynamic Effect

Based on the approach given by Fritz[5], the hydrodynamic forces of the fluid coupling, H, between the internal equipment and the building shown in Fig.1, can be written as follows :

$$\begin{Bmatrix} F_s \\ F_p \end{Bmatrix} = \begin{bmatrix} -m_H & m_I \\ m_I + m_H & -m_{II} \end{bmatrix} \begin{Bmatrix} \ddot{x}_s \\ \ddot{X}_p \end{Bmatrix} \tag{1}$$

where

F_p : Force acting on the pool structure by the submerged equipment movement

F_s : Force acting on the submerged equipment by the pool structure movement

m_H : Hydrodynamic mass associated with the submerged equipment

m_I : Mass of fluid displaced by the submerged equipment

m_{II} : Mass of fluid which would be enclosed by the pool structure without the submerged equipment

x_s : Motion of the submerged equipment relative to the pool structure

X_p : Absolute motion of the pool structure

For the dynamic analysis of interaction between the submerged internal equipment and the building, a cylindrical piece of equipment having a solid or hollow square cross-section is chosen. The equipment is assumed to be fully submerged in a rectangular pool which is located in a building. Sloshing effect of the contained fluid to the seismic response of submerged equipment or building pool structures is assumed to be negligible. Fluid coupling between the submerged equipment and rigid wall of the pool is caused entirely by the inertia of the fluid which is assumed to be incompressible and inviscid.

For a normal hexahedron with a square cross-section surrounded by a rigid concentric outer wall with narrow fluid gap as shown in Fig.1c, the ratio of submerged natural frequency f_{sH} of the equipment to the one in air f_s is given by[6]

$$\frac{f_{sH}}{f_s} = \frac{1}{\sqrt{1 + \frac{m_I}{24 m_s} \cdot \frac{(1+r)^3}{(1-r)r^2} \cdot \left(\frac{1}{1-e^2} + 3\right)}} \qquad \text{for } 0.5 \le r < 1, \quad e \ne 1 \tag{2}$$

where r is the ratio of the equipment width, w_s, to the pool width, w_p, given by $r = w_s / w_p$, and the eccentricity, e, is defined as the ratio of E, the equipment initial deviation from the concentric center, to the gap size, g, given by $e = E / g$. These dimensionless variables, r and e, are defined as control variables of fluid gap optimization for the reduction of submerged equipment response.

In order to simply express the interaction of a submerged equipment with the fluid, let us consider a single degree of freedom system as shown in Fig.1. In this simple system, the displacement relative to the building floor would be an important measure as an indicator of structural integrity because the relative displacement is, in general, proportional to the strain inside a structure. For a multi-story building which is base-fixed and dynamically behaves

like a simple beam[6], it can be approximately modeled as a single degree of freedom system as shown in Fig.1a. From the fact that the first mode of the base-isolated building is almost entirely a rigid body mode, in which there is no deformation in the superstructure, the base-isolated building can be simplified as 2-DOF system model consisted of the isolator at the base and the superstructure of building as shown in Fig. 1b.

2. 2 Equation of Motion for the Coupled System

Dynamic models of submerged internal equipment located on buildings with two different base conditions are shown in Fig. 1a and Fig. 1b. The base-fixed building has a lumped mass M_p, a stiffness K_p, a damping coefficient C_p, and the submerged equipment has mass m_s and stiffness k_s, a damping coefficient c_s as shown in *Fig. 1a*. Hydrodynamic coupling H between the internal equipment and the pool structure on the building is modeled using equation (1). Let U_g, U_p, and u_s be respectively the ground motion, displacement of the building structure to the base, and that of the submerged equipment relative to the building floor. Then, the equations of motion for the internal equipment in base-fixed building model become

$$\begin{aligned} M'\ddot{U}_p + C_p\dot{U}_p + K_pU_p &= -M'\ddot{U}_g - m_{sI}\ddot{u}_s \\ m_{sH}\ddot{u}_s + c_s\dot{u}_s + k_su_s &= -m_{sI}(\ddot{U}_g + \ddot{U}_p) \end{aligned} \tag{3}$$

where $M' = M_p + m_H + m_{sI}$, $m_{sI} = m_s - m_I$, $m_{sH} = m_s + m_H$.

Now let us assume the building is base-isolated. And the base is assumed to have mass M_b, stiffness K_b, a damping coefficient C_b. Let U_b be the base displacement relative to the ground and other assumptions and notations be the same as in the case of base-fixed building. Then the equations of motion for the total system are given by

$$\begin{aligned} M'\ddot{U}_b + C_b\dot{U}_b + K_bU_b &= -M'\ddot{U}_g - M'\ddot{U}_p - m_{sI}\ddot{u}_s \\ M'\ddot{U}_p + C_p\dot{U}_p + K_pU_p &= -M'(\ddot{U}_g + \ddot{U}_b) - m_{sI}\ddot{u}_s \\ m_{sH}\ddot{u}_s + c_s\dot{u}_s + k_su_s &= -m_{sI}(\ddot{U}_g + \ddot{U}_b + \ddot{U}_p) \end{aligned} \tag{4}$$

where $M' = M_b + M'$.

3. SEISMIC ANALYSIS AND DISCUSSION

3.1 Descriptions of Analysis Method

The fundamental natural frequency and damping ratio of the base-fixed building model in Fig. 1a are respectively assumed to be 3.3Hz and 0.02. To analyze the influence of base-

isolation type on the seismic response of the submerged internal equipment, four different types of base isolation devices ; Laminated Rubber Bearing(LRB), Pure-Friction(P-F) isolator, isolator by Electricite de France (EDF) and Resilient-Friction Base Isolation system(R-FBI) are considered. The natural frequencies and damping ratios of the base-isolators are as shown in Table 1[2]. A value of 0.01 is taken for the common mass ratio of the submerged equipment to the floor, and 0.01 for the damping ratio of the submerged equipment based on m_{sH}. The peak seismic responses are calculated for the in-air natural frequency of 0 Hz to 20 Hz.

The sixth order Runge-Kutta scheme and double precision were chosen for numerical integration of the equations of motion in FORTRAN. The input earthquake is El Centro 1940. Since displacement of the submerged equipment relative to the floor would be an indicator of strain in real elastic structures, the response of the equipment is discussed mainly in terms of the relative displacement response.

3.2 Influences of Building Base-Isolation on Equipment Response

Fig. 2 shows two different effects of the building base-isolation on the seismic responses of internal equipment in air and in submerged condition. The peak seismic responses of the internal equipment for f_s = 0 Hz - 20 Hz are investigated. As reported from many studies, both of the EDF and LRB building base-isolations significantly reduce the seismic response of the in-air equipment regardless of the natural frequency of the equipment for f_s = 1.5 Hz - 20 Hz as shown in Fig.2a. On the contrary, the base-isolation of the building turns out to give adverse effect on the response of the submerged equipment. Fig. 2b shows amplification of the peak responses of the submerged internal equipment by EDF or LRB base-isolation of the building for the added mass effect $\frac{m_{sH}}{m_s}$ = 64. It can be seen that in the EDF and LRB base-isolations the response rises near the submerged resonance frequencies f_{sH} = 0.9 Hz and 0.5 Hz respectively, which correspond to f_s = 7.5 Hz and 4 Hz for $\frac{m_{sH}}{m_s}$ = 64. That is, the response increase at the resonance peak for the LRB and EDF base-isolations and the level of increase is about 4 to 6 times at worst cases.

Fig.3 shows the effect of building base isolation on the peak sliding displacement of the submerged internal equipment for the added mass effect $\frac{m_{sH}}{m_s}$ = 25 when the equipment is assumed to be free standing and the friction coefficient to be a value of 0.2. Though the increase or decrease of the peak responses depends upon the natural frequency of the equipment, the maximum increase of the sliding displacement reaches about 4 times. Considering that the peak sliding displacement is one of the important factor in seismic design for the free standing equipment, the adverse effect on the submerged equipment by building base isolation should be overcome through an appropriate design strategy.

3.3 Response Reduction by Fluid Gap Optimization

In order to prevent the submerged internal equipment from resonating with the base-isolated building, an appropriate control of the hydrodynamic effect can be attempted. The hydrodynamic effect can be controlled by adjusting the fluid gap size and initial location of the equipment relative to the surrounding structure. Because this adjustment can be practical after the design constraints such as possibility of collision with adjacent structures and minimum space required for interfacing systems are evaluated, optimization of fluid gap was made with those constraints. And the possible range of fluid gap is assumed to be 0 to 25 cm for analysis purpose in this case.

Fig. 4 shows the level of response reduction by the gap optimization. The original peak displacements are calculated for the added mass effect $\frac{m_{sH}}{m_s} = 25$, which corresponds to a constant fluid gap condition. Then, the fluid gap can be determined to minimize the peak responses of the submerged equipment for each cases by optimization. The minimized responses and the corresponding optimal gaps of equipment in base-fixed building are shown in Fig. 4a. The optimal gap turns out to be constantly 0.5 or 1.0 cm, which is almost the lower bound, regardless of the natural frequency. The response reduction can be obtained in the level of about 1/4 - 1/40 throughout the frequency range. In LRB base-isolated building, the optimal gap varies fully within the range of 0.5 cm to 25 cm to minimize the response. The effect of response reduction, the maximum level of which is about 1/20, is noted for $f_s < 5.0$ Hz, while it is negligible for $f_s > 5.0$ Hz because the response has already decreased much for the range.

3.4 Response Reduction by Base Isolation of Submerged Equipment

In case that the level of response control by fluid gap optimization is limited, application of base-isolation simultaneously to the submerged equipment may be an alternative. If the submerged equipment is subject to a considerable hydrodynamic effect, the added mass effect will help to prevent the base-isolated equipment resonating with floor excitations in the base-isolated building. Thus, the fundamental frequency of the base-isolated submerged equipment becomes much lower than that of the base-isolated building.

As reviewed and discussed in section 3.2, the seismic response of the submerged equipment can be highly aggravated by EDF or LRB base-isolation of the building structure. To get the best combination between the base-isolators for the building structure and the base-isolators for the submerged equipment, the seismic responses of the equipment in five different base conditions are analyzed and compared. In Fig. 5, the peak acceleration and displacement responses are compared for the equipment base-isolation using four different types in EDF base-isolated structure. For the case of EDF base-isolated building structure, EDF base-isolation of the submerged equipment shows the least and constant absolute acceleration response as shown in Fig. 5a, and LRB base-isolation of the equipment does the least relative displacement as shown in Fig. 5b.

The peak acceleration and displacement responses of the submerged equipment with the LRB base-isolated building structure are shown in Fig. 6a and Fig. 6b. Even though the response amplitudes are slightly different, the overall trends for the internal equipment isolators are quite similar to those for EDF isolation, that is, EDF base-isolation of the submerged equipment shows the best performance for the acceleration response attenuation

and LRB base-isolation of the submerged equipment shows the best for the displacement response attenuation of the system.

4. CONCLUSIONS

When base isolation is applied to the building structure, the main frequency components of the floor vibrations of the building structure are shifted to low range, and hence, hydrodynamic effects on the equipment, which are very desirable in base-fixed building structures, bring about adverse effects. Therefore, in the base-isolation design of building structures on which submerged equipment are installed, great care should be taken so that there might not occur resonance of the submerged equipment with the fundamental natural frequency of the building structure. In summary,

1) The peak displacement response of the submerged internal equipment, which is subject to a considerable hydrodynamic effect, can be significantly increased by the base-isolation in the building structure while the response of the in-air equipment decreased.

2) By an optimization of the fluid gap, the seismic response of the submerged equipment can be largely reduced. Closer fluid gap with no impact possibility turns out to be better in base-fixed structure, but the optimal size of fluid gap is largely dependent on the equipment natural frequency in base-isolated structure.

3) The LRB or EDF base-isolation of the submerged equipment can remarkably reduce the seismic response by using the hydrodynamic mass effect for further lowering the natural frequency of the equipment, and it can be a good alternative in the case where the response reduction by fluid gap design is limited.

REFERENCES

1. Tsai, H., J. M. Kelly 1989. Seismic response of the superstructure and attached equipment in a base-isolated building. *Earthquake Eng. Struct. Dyn.* 18: 551-564.

2. Fan, F., G. Ahmadi 1992. Seismic response of secondary systems in base-isolated structures. *Eng. Struct.* 14: 35-48.

3. Singh, S., S. F. Putman & J. Pop 1990. Structural evaluation of onsite spent fuel storage: recent developments. *3rd Symposium on Current Issues Related to Nuclear Power Plant Structures, Equipment and Piping* : V/4-1-V/4-18. Orlando: Florida.

4. Scavuzzo, R., W. F. Stokey & E. F. Radke 1979. Dynamic fluid-structure coupling of rectangular pools. *ASME PVP*-39: 77-86.

5. Fritz, R. 1972. The effect of liquids on the dynamic motions of immersed solids. *J. eng. ind. Trans. ASME*: 167-173.

6. Shin, T., K.J. Kim 1996. Seismic response amplification of submerged secondary system in base-isolated structures. *CST96 3rd Int. Conf. On Computational Structural Technology*: 269-281. Budapest: Hungary.

Table 1. Values of model parameters used for various base-isolators

Base Isolation System	Natural Frequency f_u (Hz)	Damping Ratio ξ_u (Loss Factor)	Friction Coeff. μ
Laminated Rubber Bearing (LRB)	0.5	0.08 (0.16)	-
Pure-Friction (P-F)	-	-	0.1
Resilient-Friction (R-FB1)	0.25	0.08(0.16)	0.05
Electricite De France(EDF)	1.0	0.08(0.16)	0.2

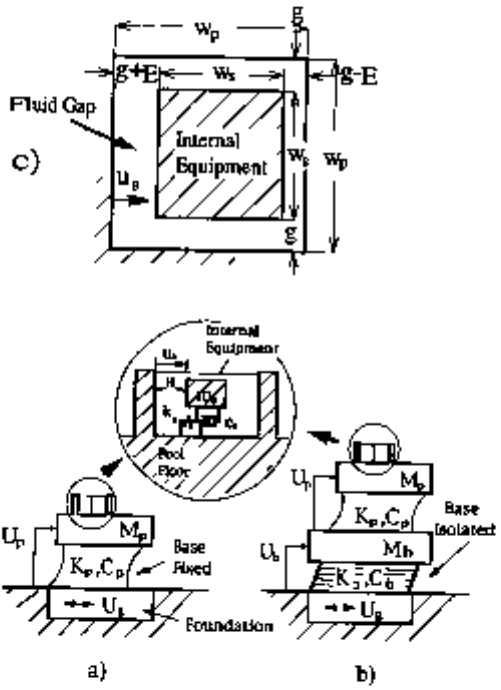

Fig. 1 Coupled model of submerged equipment
a) on base-fixed building,
b) on base-isolated building

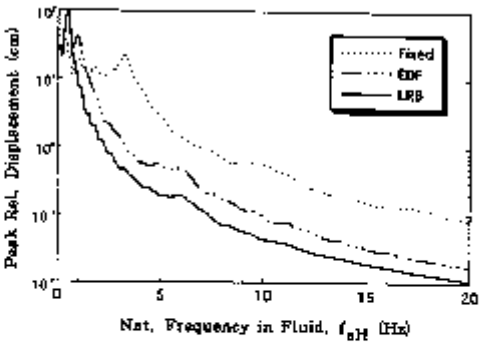

a) In-Air Internal Equipment

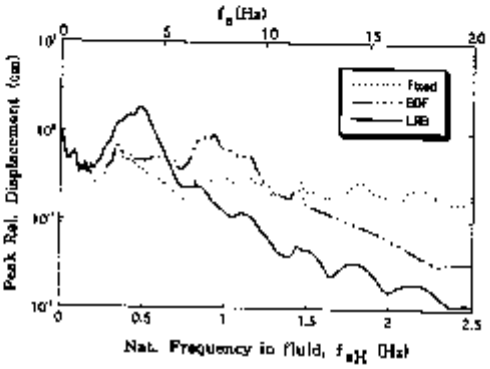

b) Submerged Internal Equipment (m_{sH}/m_b=64)

Fig. 2 Effect of building base isolation on the peak responses of submerged equipment

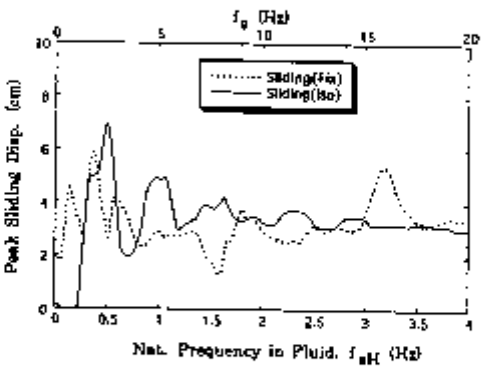

Fig. 3 Effect of building base isolation on the peak sliding displacements of submerged equipment at f_{sH} = 0 - 4 Hz

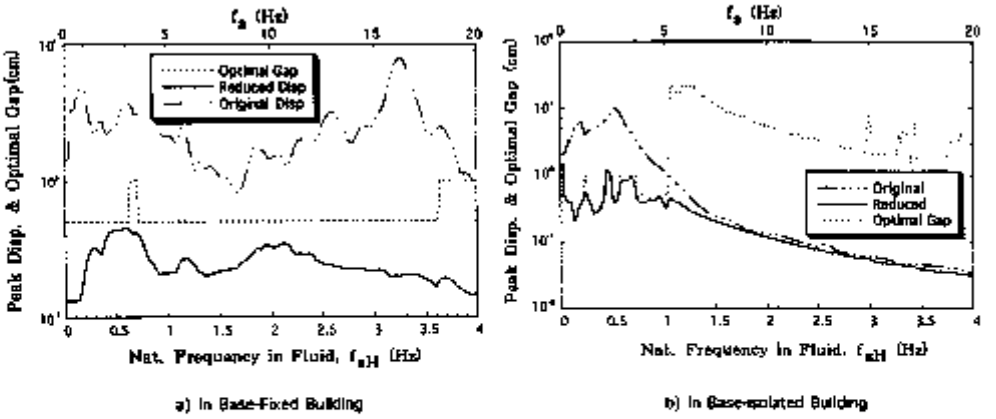

Fig. 4 Response reduction of submerged equipment at f_{sH} = 0 - 4 Hz by fluid gap optimization

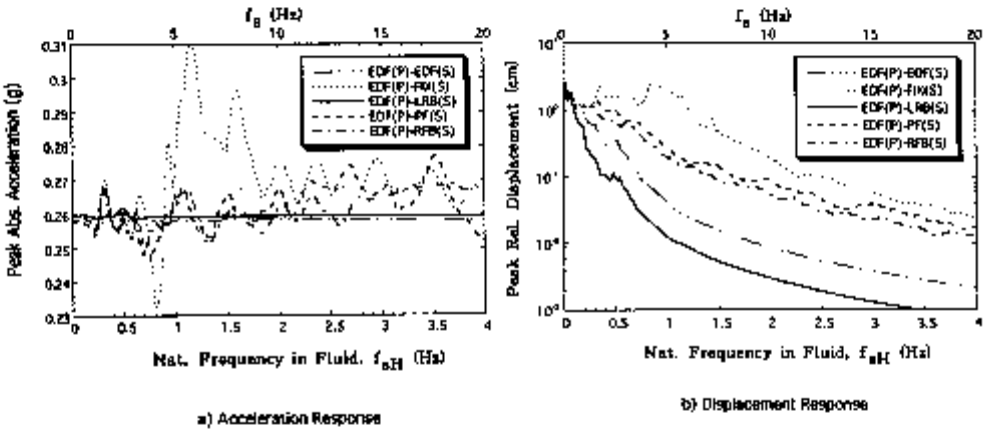

Fig. 5 Peak responses of base-isolated equipment in EDF base-isolated building at f_{sH} = 0 - 4 Hz

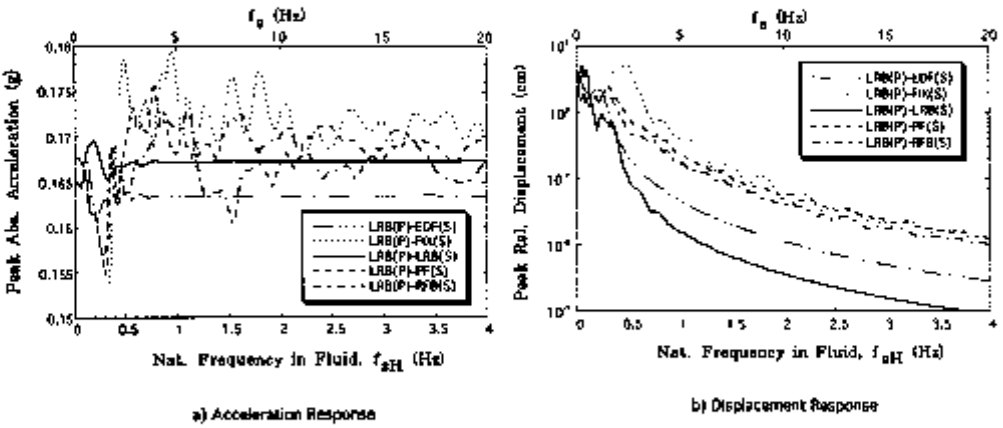

Fig. 6 Peak responses of base-isolated equipment in LRB base-isolated building at f_{sH} = 0 - 4 Hz

Transactions of the 14th International Conference on Structural Mechanics in Reactor Technology (SMiRT 14), Lyon, France, August 17-22, 1997 K20/4

Pseudo-dynamic test and nonlinear numerical simulation of isolated structure

Kim S.H.
Korea Power Engineering Company, Korea

Abstract

A computer code based on the finite element method has been developed for analyzing the response of isolated structure subjected to the dynamically excited loading induced by the operation of machines or the earthquake. A finite element program has the four different elements; beam, plate/shell, boundary spring and spring elements. The spring element represents the seismic or vibration isolator that is used to lower the fundamental frequency of structure, and thus it would take a large portion of nonlinear deformation of structures. As result, the spring element only is considered to be nonlinear in the program. In order to verify the performance of the developed code, the pseudo-dynamic tests of an isolated steel structure under two different earthquakes have been carried out. The layered rubber springs are used as the isolation devices, of which mechanical behavior is assumed to be bi-linear, and the mechanical properties are obtained from the experiments. Non-linear responses of an isolated steel structure subjected to two different earthquakes are simulated and compared with the results of pseudo-dynamic tests. Simulations of structural responses show good agreement with the results of the pseudo-dynamic tests.

1. Introduction

If a program is developed for analyzing the structural responses caused by seismic, shock, and vibration loading, it may be necessary that the program be evaluated by comparing the numerical results with those of experimental tests. In the study a program is coded on the base of the finite element method to estimate the nonlinear dynamic responses of isolated structures, and its validity is evaluated by the pseudo-dynamic tests of isolators, LRB(Layered Rubber Bearing), and a proper test model of isolated structure.

The finite element program includes three types of element which are the most common elements in analysis of structures; beam, plate/shell and spring elements. The spring element represents the isolator and it only is considered to be nonlinear. The reason is that its stiffness is the smaller than that of other element. The isolator shifts down the fundamental frequency to less than the frequency spectrum of the dynamic loading[1]. The stiffness matrix of spring element in the study is formulated by using the bi-linear load-deflection relation and the kinetic hardening rule, which are reflected from the experimental hysteretic loops.

The pseudo-dynamic test are carried out after investigating the mechanical properties of LRB under the various conditions such as the maximum shear strain, the vertical loads and the loading rates. Three sizes of LRBs are fabricated and tested to prove the similitude rule

and to observe the static properties. The equivalent stiffness and the effective damping ratios can be obtained from the hysteretic load-displacement loops, and they are used as the input of the finite element program to directly construct the stiffness matrix of isolator.

A five-story two-bay steel building is chosen to evaluate the home made program NAIS (Nonlinear Analysis for Isolated Structure) through the pseudo-dynamic test[2,3]. The pseudo-dynamic test is more economical method, utilize the conventional laboratory test equipment and permit the detailed observation of specimens during test. It is well known that a pseudo-dynamic test model is combination of the actual structural model to be tested and the numerical model which does not exist. LRBs of the steel structure in tests are the actual structural elements, while the superstructure above isolators is replaced by the numerical models. The seismic responses caused by El Centro and Taft earthquakes are measured by the pseudo-dynamic test and they are simulated by NAIS, and two results are compared.

2. Non-linear Finite Element Analysis

Since the stiffness of isolator could be so small compared with that of any structural member, the natural frequency of isolated structure is far less than that of the un-isolated structure. If the earthquake excitation or the machine load are enough for nonlinear behavior of isolated structure, it may be due to isolator as expected.

As a result, a nonlinear finite element program has been coded not only for the estimation of the structural behavior but also for the design of isolated foundation of structure and machine. In the section, one describes the formulation of stiffness matrix of the spring properties element in the finite element program.

The potential energy of structure can be expressed as

$$\Pi = \int_V \sigma\varepsilon \, dV - \int_V \mathbf{u}(\mathbf{f}_b - \rho\ddot{\mathbf{u}} - c\dot{\mathbf{u}}) \, dV \quad - \int_V \mathbf{u}\mathbf{q} \, dV$$

in which $\mathbf{f}_b$ is the body force, ρ is the density, c the damping coefficient, and $(\bullet)$ indicates the derivatives with respect to time. Thus $\ddot{\mathbf{u}}$ and $\dot{\mathbf{u}}$ represent the acceleration and the velocity, respectively. By applying the principle of virtual work, the equation of motion then can be written as

$$\mathbf{M}\ddot{\mathbf{u}} + \mathbf{C}\dot{\mathbf{u}} + \mathbf{K}\mathbf{u} = \mathbf{F}$$

where $\mathbf{M}, \mathbf{C}, \mathbf{K}$ are the matrices of mass, damping and stiffness, respectively. The matrices in the finite element analysis can be expressed in a form

$$\mathbf{M} = \int_V \mathbf{N}^T \rho \mathbf{N} \, dV, \quad \mathbf{C} = \int_V \mathbf{N}^T c \mathbf{N} \, dV, \quad \mathbf{K} = \int_V \mathbf{B}^T \mathbf{D} \mathbf{B} \, dV$$

in which $\mathbf{N}$ is the interpolation matrix, $\mathbf{B}$ is the strain displacement matrix, and $\mathbf{D}$ is the stress-strain relation or moduli matrix dependent upon the type of element.

A nodal point in the spring element has 6 degree of freedom same as beam element; Three (u, v, w) are from the translation, and the three $(\theta_x, \theta_y, \theta_z)$ are from the rotation. In the study, a spring element is composed of 2 nodes, and thus the rank of stiffness or mass matrix is 12.

The nodal displacement vectors can be expressed as

$$\mathbf{u}^T = [u \; v \; w \; \theta_x \; \theta_y \; \theta_z]$$

and the corresponding nodal force vector can be written as

$$\mathbf{f}^T = [f_x \; f_y \; f_z \; m_x \; m_y \; m_z]$$

where m_i denotes the moment about the i-axis in the local coordinate. If the nodal variables

are assumed to be uncoupled, the force vector can be determined by the difference of displacements at two nodes in element, and the relationship between the nodal force vector and the nodal displacement vector can be established as

$$f_k = k_k(u_{kj} - u_{ki})$$

where the subscript k denotes the k^{th} degree of freedom in element. The local coordinate system of spring element is defined as the similar manner for beam element. The stiffness matrix of spring element can be expressed

$$\mathbf{K} = \begin{bmatrix} \mathbf{K}_s & -\mathbf{K}_s \\ -\mathbf{K}_s & \mathbf{K}_s \end{bmatrix}, \quad \mathbf{K}_s = \begin{pmatrix} k_x & 0 & 0 & 0 & 0 & 0 \\ 0 & k_y & 0 & 0 & 0 & 0 \\ 0 & 0 & k_z & 0 & 0 & 0 \\ 0 & 0 & 0 & k_{\theta x} & 0 & 0 \\ 0 & 0 & 0 & 0 & k_{\theta y} & 0 \\ 0 & 0 & 0 & 0 & 0 & k_{\theta z} \end{pmatrix}$$

As mentioned before, the rank of stiffness matrix of spring element is 12, the stiffness in $\mathbf{K}_s$ are directly formulated by the input stiffness.

3. Pseudo-Dynamic Test

For the safety and integrity of structure, the dynamic behavior of structure at the stage of the conceptual design has been experimentally observed using the appropriate test methods such as the shaking table test, the pseudo-dynamic test and so on. If the structure in the nuclear power plant are designed by introducing new concepts, the prototype or the scale model of structure should be tested in order to investigate its dynamic properties and behaviors under the severe loading conditions such as earthquake motions.

The quasi-static test method has been used to investigate the nonlinear characteristics of the whole or the parts of structures. The method is simple and is adopted independent of the size of structure, but the dynamic effects may not be well reflected because the nonlinear force-deformation characteristics of structure should be known or assumed before testing.

In 1969 the pseudo-dynamic test method was introduced by Takanashi[4] for investigating the large structure under the seismic ground motions. Since the test is the combination of the shaking table test and the quasi-static test, the test facility is relatively more simple than that of the shaking table test, but the testing results may be comparable to the results of the shaking table test. Also, the pseudo-dynamic test is relatively inexpensive method when the full-scale structure is tested, because the structural elements whose mechanical properties are not well defined are tested actual but the remaining structural elements are modeled numerically. The mechanical properties of elements numerically modeled are considered to be well defined rather than the elements subjected to the actual forces.

The pseudo-dynamic test constitutes of two parts; One is the computational part and the other is the experimental part under the actual forces, as shown in Fig. 1. The computational part can be performed by the computer, and the experimental part includes the servo valves, load cells, and/or oil pressure transducers. The reaction forces from the structure are measured by load cell and used as the input of the numerical integration via the data acquisition system by which the analog signal are filtered and converted to the digital signal. The structure then is deformed by actuator as much as displacement from the numerical integration.

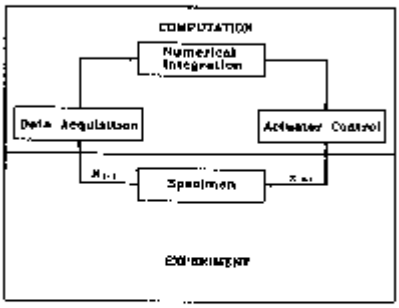

Fig. 1 Schematic Diagram of Pseudo-Dynamic Test

Since the explicit time integration scheme is adopted in test, the equation of motion is solved corresponding to the restoring force which is measured on the structure, and also the stiffness matrix are established at every time step. The computational procedure[5] are as follows;

1. Calculate the initial condition using equation,

$$\ddot{\mathbf{x}}_0 = \mathbf{M}^{-1}(\mathbf{F}_0^e - \mathbf{F}_0^i)$$

2. Evaluate the displacement using the equation

$$\mathbf{x}_{n+1} = \mathbf{x}_n + \Delta t\,\dot{\mathbf{x}}_n + \frac{\Delta t^2}{2}\ddot{\mathbf{x}}_n$$

3. Impose the displacement $\mathbf{x}_{n+1}$ on the structure to be tested.
4. Measure the restoring force $\mathbf{R}_{n+1}$ at the designated points of structure.
5. Correct the restoring force
6. Compute the acceleration and the corresponding using the equations

$$\ddot{\mathbf{x}}_{n+1} = \left(\mathbf{M} + \frac{\Delta t}{2}\mathbf{C}\right)^{-1} \cdot \left(\mathbf{F}_{n+1} + \mathbf{R}_{n+1} - \mathbf{C}\dot{\mathbf{x}}_{n+1} - \frac{\Delta t}{2}\mathbf{C}\ddot{\mathbf{x}}_n\right), \quad \dot{\mathbf{x}}_{n+1} = \dot{\mathbf{x}}_n + \frac{\Delta t}{2}(\ddot{\mathbf{x}}_{n+1} + \ddot{\mathbf{x}}_n)$$

7. If the step n is less than the total number of steps N, return to 2 after setting $n = n+1$. Otherwise, stop.

The steps 3 and 4 are included in the experimental part as mentioned before, and others are included in the numerical part.

4. Experimental Tests of LRB

The cylindrical LRBs whose diameters are 75, 150 and 300 mm are designed and fabricated for investigating the similitude rule and the effective damping ratio and the equivalent stiffness under various conditions. The schematic shape are shown in Fig. 2 and the their specification are listed in Table 1. Table 2 shows the mechanical properties of rubber, and Table 3 shows the design values of stiffness and buckling loads of three LRBs.

Fig. 3 shows the schematic diagram of LRB test equipment and facility. Two hydraulic actuators are used to apply loads in the horizontal and vertical directions simultaneously. The capacities of vertical actuator which controls the vertical load are $\pm 50ton$ and $\pm 125mm$, and those of horizontal actuator which controls the shear deformation are $\pm 25ton$ and $\pm 125mm$.

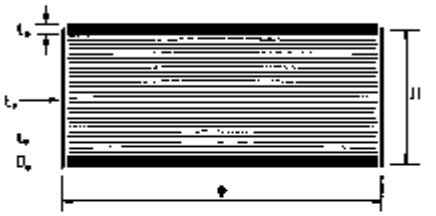

Fig. 2 LRB being tested; Φ: diameter, H: height, D_s: diameter of steel plate, t_r and t_s: thickness of rubber and steel plate, t_e :thickness of end plate, n: number of layers

Table 1 Dimensions of LRB(unit:mm)

	Type I	Type II	Type III
Φ	150	75	300
H	87	64.9	147
D_s	142	71	284
t_r	3.7	1.85	7.4
t_s	2	1.6	3
n	16	16	23
t_e	10	10	10
scale	1/2	1/4	1

Table 2 Material Properties of Synthetic Rubber

shear modulus	G = 1.0 MPa
bulk compressive modulus	E_0 =1.0 GP
apparent compressive modulus	E_c = 0.87 GPa
Poisson's ratio	ν =0.5
chemical parameter	β = 3.53

Table 3 Designed Stiffness and Buckling Load

	vertical stiffness (ton/cm)	horizontal stiffness (ton/cm)	rotational stiffness (ton-cm/rad)	buckling load (ton)
Type I	225.15	436.75	1376.20	75.06
Type II	112.58	218.38	171.65	12.56
Type III	450.31	873.51	10985.6	301.4

The load-displacement relation in the vertical direction is shown in Fig. 4. The vertical stiffness from this test is about 193.88 *ton/cm*, while the designed vertical stiffness in Table 3 is 225.15 ton/cm. Hence the difference between two results is 13.9%, which is considered to be in the acceptable range. The offset in Fig 4. is considered to be due to the loose of test fixture.

The horizontal hysteretic loops dependent upon the maximum shear deformation are shown in Fig. 5, and the effective stiffness and the damping ration with respect to the maximum shear strain are shown in Fig. 6. The horizontal hysteretic tests are carried out under the constant vertical load of 11.2 ton. As shown in Fig. 5, the stiffness varies dependent upon load, and thus the enough interval between subsequent tests were provided for the settlement.

Fig. 5 shows that the stiffness increases at the tips of hysteretic loops if the maximum shear strain are more than 150%. But the phenomena do not appear for relatively small strain.

Fig. 7 shows the stiffness and the damping ratio referring to the rate of load in the range of 0~2Hz. The effective stiffness gradually increases with the loading rate, and the effective damping ratio also increases with rather lager slope than stiffness.

It is considered that the effective stiffness and the effective damping ratio as shown in Fig. 8 are not much affected by the vertical loads.

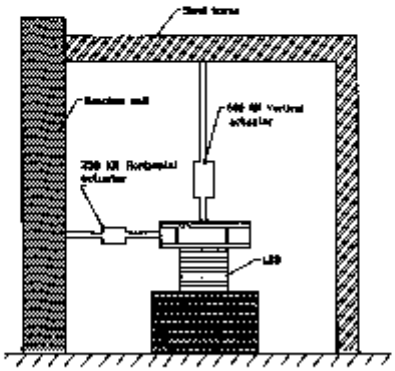

Fig. 3 Testing Machine

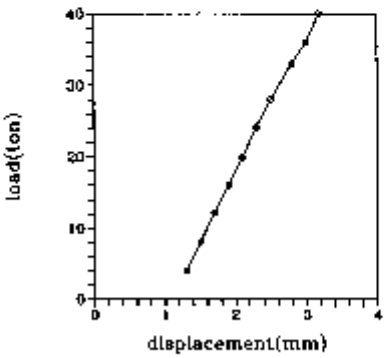

Fig. 4 Vertical Load-Displacement Relation

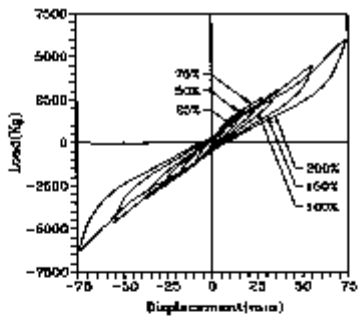

Fig. 5 Hysteretic Loops According to Maximum Shear Strains

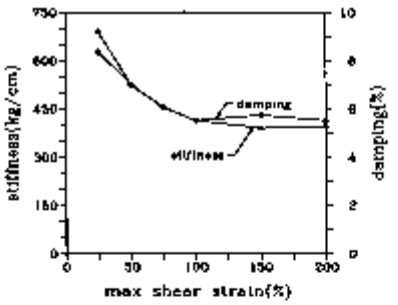

Fig. 6 Equivalent stiffness and effective damping ratio

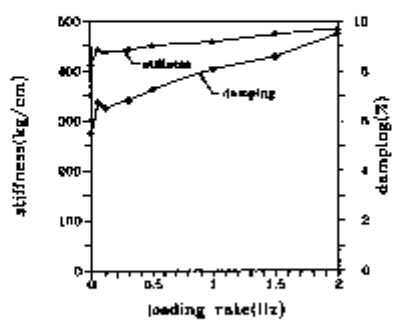

Fig. 7 Equivalent stiffness and effective damping ratio with respect to loading rate

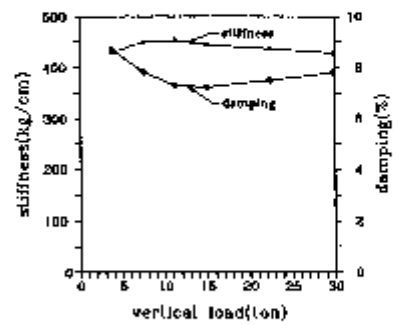

Fig. 8 Equivalent stiffness and effective damping ration with respect to vertical load

5. Numerical Simulations and Pseudo-Dynamic Tests

Two-bay five-story steel building as shown in Fig. 9 are chosen to evaluate the home made finite element analysis program NAIS through the pseudo-dynamic tests. The behaviors of steel structure subjected to the two different earthquake excitations, El Centro and Taft, are simulated by NAIS and are observed by the pseudo-dynamic tests.

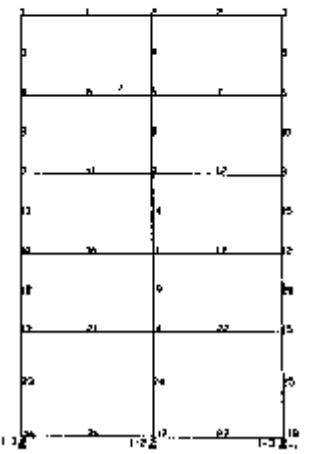

Fig. 9 Finite element model of isolated steel building

In experimental tests, the isolators LRB are real but the rest of structure is modeled by the finite element model as defined in the fundamental of pseudo-dynamic test. The nodal displacements calculated by computer are imposed to the designated points of structure using the hydraulic actuator, and the reaction measured by load-cell is used as the input of a numerical program which is different from NAIS.

In the finite element analysis, the number of nodes can be determined by the expected behavior of structure. The nodes of the finite element model are located at the junction points as shown in Fig. 9, because the fundamental frequency of steel elements is far less than the major frequency spectrum of excitations. The recommended minimum number of nodes to be placed along the members should be larger than the number of mode of a simply supported beam. As a result the computational efforts can be reduced. The super structure model are supported by three LRB isolator as indicated I-1, I-2 and I-3. The finite element model is composed of 31 nodes, 27 beam elements and 3 spring elements as shown in Fig. 9.

The load-displacement relation of spring is assumed to be bi-linear which can be determined by elastic and elasto-plastic stiffnesses and yield strength. Since the stiffness of LRB depends upon the shear strain, the behavior of isolated structure can not be estimated precisely by one simulation. Thus at least two numerical simulations should be required to determine two stiffness and yield strength.

Taft and El Centro earthquakes are adopted as the base motion of experimental tests and numerical simulations. The seismic responses from the numerical simulations are agreed well with those of pseudo-dynamic tests as shown in Fig. 10 and 11. Therefore, it is considered that the computer program NAIS can be useful to simulate the dynamic responses of isolated structure with accuracy.

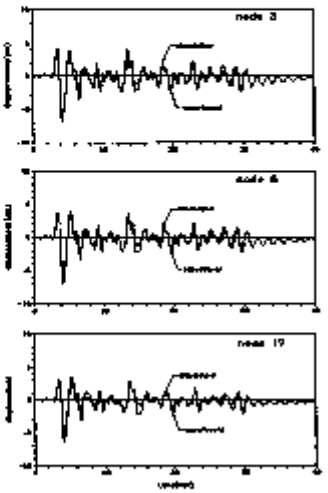

Fig. 10 Responses of earthquake Taft

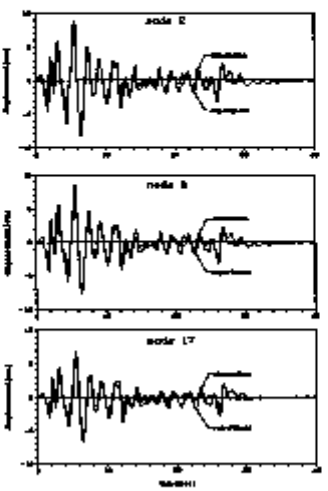

Fig. 11 Responses of earthquake El Centro

6. Conclusion

A finite element program NAIS for analyzing the dynamic nonlinear behavior of isolated structures has been verified through the pseudo-dynamic tests of a isolated steel structure subjected to two earthquake motions, and the program could be useful for the analysis of the dynamic behavior appropriately.

References

[1] Kunar, R.R., " A Review of Seismic Isolation for Nuclear Structures," EPRI Special Report, NP-1220-SR, Oct., 1979.

[2] Shing, P.B., Mahin, S.A., "Pseudodynamic Test Method for Seismic Performance: Theory and Implementation", EERC, Report, UBC/EERC-84/01, 1984.

[3] Mahin, S.A. and Shing, P.B., "Pseudo-dynamic Method for Seismic Testing", J. of Structural Engineering, ASCE, Vol. 111, No. 7, 1985.

[4] Takahashi, T. et al, "Seismic Failure Analysis of Structures by Computer -Pulsator On-Line System", Bull. of Earthquake Resistant Structure Research Center, Institute of Industrial Science, University of Tokyo, No. 11, 1974.

[5] Kim, S.H., " A Study on the Optimal Design of Structure with the Application of Isolation Devices", Korea Power Engineering Co. Inc., Report, KOPEC/95-T-106, Dec., 1995.

Transactions of the 14th International Conference on Structural Mechanics in Reactor Technology (SMiRT 14), Lyon, France, August 17-22, 1997

Seismic failure probability evaluation of FBR equipment on an isolated plant

Sekiya H.[1], Kamishima Y.[2], Tanaka K.[3]
(1) Mitsubishi Heavy Industries, Japan
(2) Advanced Reactor Technology Company, LTD, Japan
(3) Tokyo Electric Power Company, Japan

ABSTRACT : A fragility assessment based on safety factors was carried out for major equipment in a base-isolated Fast Breeder Reactor (FBR) plant.
The authors propose a method for evaluating the non-linear response factor of an isolated building and the capacity factor of the equipment subjected to the modified seismic accelerations. The results show that the hardening point of the isolation devices ,i.e., the skeleton of the rubber bearings is dominant in the failure probability and the shape of the fragility curve.

1. INTRODUCTION

In the design of a FBR, the application of a seismic isolation system is effective for reducing the seismic loads which are critical to the structural design of equipment. [1] From the safety point of view, however, the impact of the application on overall plant safety should be examined using quantitative methods such as a seismic probabilistic safety assessment (PSA). In the seismic PSA the failure probabilities of equipment are calculated as a function of input acceleration.
Although a base-isolated building responds almost linearly for design level inputs, the response shows a non-linear tendency after the isolation system i.e. the rubber bearings are displaced beyond a hardening point. Therefore particular consideration should be given to dealing with this non-linearity since the previous safety factor method has been based on the assumption that the building will respond linearly.
In this study, a fragility assessment based on response and capacity factors was carried out for the reactor vessel (RV) taking account of the non-linearity of the isolation system.

2. DESIGN DESCRIPTION

2.1 Base-isolated building

The FBR plant is base-isolated in the horizontal direction. [1] The isolation system is composed of natural rubber bearings and steel dampers. The design specification of the base-isolation system is as follows:

Horizontal	Initial period T_1	1.0 sec	
	Isolated period T_2	2.0 sec	
	Yield coefficient	0.05	
Vertical	Natural period	0.05 sec	
Supporting load		750 ton	(per rubber bearing)
Rupture displacement		68.9 cm	
Displacement for S_2 earthquake		14.0 cm	

2.2 Reactor vessel

The RV is installed at the level in the base-isolated building shown in Fig. 1. The RV has a diameter of 10.4 m and a thickness of 35 mm. Its natural frequency for a single degree of freedom is 5 Hz horizontally and 11.6 Hz vertically. The effective mass W is 2000 ton and the damping factor is 0.01. The stress on the RV σ_{RV} induced by the seismic loads can be expressed by:

$$\sigma_{RV} = \sigma_b + \sigma_n = \frac{M}{Z} + \frac{F}{A} \qquad (1)$$

where M: Bending moment = $L_m \times W \times \alpha_H$ (horizontal acceleration)
F: Axial force = $W \times \alpha_V$ (vertical acceleration)

3. OUTLINE OF FRAGILITY ANALYSIS

The fragility ,e.g., the conditional frequency of failure P_f for a given peak ground acceleration (PGA) level, a, is generally given by three constants, i.e., median ground acceleration A and logarithmic standards β_R and β_U [2]:

$$P_f = \Phi\left[\frac{\ln\left(a/\breve{A}\right) + \beta_U \Phi^{-1}(Q)}{\beta_R}\right] \qquad (2)$$

where $\breve{A} = F \times A_{S_2}$
Φ : Standard Gaussian cumulative distribution function

The particular features of the fragility analysis are as follows:

(1) The non-linear response factor is defined as a function of PGA, a.
(2) Consequently the safety factor F and $\breve{A}$ (= F $\times S_2$) become functions of PGA, a.
(3) The uncertainty of the response caused by the variabilities in the building and isolation system are calculated at several input levels. However an enveloped value is applied to the response factor for simplicity and conservatism.
(4) The spectral shape of the input motion is assumed to be the design earthquake S_2.
(5) Buckling is considered as the failure mode of the RV.

4. RESPONSE ANALYSIS OF THE ISOLATED BUILDING

4.1 Non-linearity characteristics

(1) Objectives
Analyses were made to evaluate the tendency to non-linearity in the response of the base-isolated building and its impact on the response of the RV.

(2) Analytical condition
The analytical model of the isolated building is shown in Fig. 1. The model is a single-stick lumped mass model which both the isolation layer and the soil-structure interaction are considered as springs. The effect of slippage of the rubber bearings was also considered. The design earthquake (S_2) has a peak acceleration of 0.388 G. Vertical motion is assumed to be 0.6 times the horizontal motion. By amplifying the input motion, the response of the isolated building were analyzed for the several input levels between S_2 and 3.5 $\times S_2$.

(3) Analysis results
Fig. 2 shows the floor response spectra (FRS) at the level where the RV is installed. The horizontal FRS for higher inputs (over 2×S2) show low-period peaks due to the non-linearity of the isolation system. This is because the displacement of the rubber bearings exceeds their linear range.
Fig. 3 shows the acceleration of the floor at the level of RV. Fig. 4 shows the displacement and shear force of the isolation system. It is clear that the building responds linearly until the input increases to 2 times the S_2 earthquake, however it's response increase drastically once the isolation system is displaced beyond the limit of linearity, i.e., the hardening point.

4.2 Uncertainty of responses

(1) Objectives
Analyses were made to evaluate the uncertainty in the responses of the base-isolated building based on a two-point estimation method.

(2) Analytical condition
The uncertainty of the responses were evaluated at S_2, $2.5\times S_2$, $3\times S_2$. The variability in the soil springs, rubber bearings, steel dampers and skeleton of the concrete were considered to evaluate the uncertainty of the responses. (Fig. 1)

(3) Analysis results
Fig. 5 shows the COV of the FRS at RV equipped level. The level of COV increases as the input level increase because of the nonlinear response of the building. The COV is however less than 0.3 at these input levels and for the range of periods close to the RV natural frequency.

5. FRAGILITY ANALYSIS OF THE REACTOR VESSEL

5.1 Response factors

(1) Spectral factor F_{SA}
This factor represents the variability in the input motion and the associated ground response spectra. As mentioned in 3.1 (3) , a uniform hazard spectrum is assumed to be same as the S_2 spectrum. Therefore F_{SA}=1.0 and β_R=0.3 for the response variability due to the variability in the input motion.

(2) Non-linear response factor F_{NL}
This factor represents the nonlinear response of the base-isolated building. Fig. 6 shows the normalized stress on the RV K_{NL}. The value of more than 1.0 for the large input level over 2 times S_2 implies a non-linear response of the base-isolated building. Thus F_{NL} was estimated to be $1/K_{NL}$ and β_U=0.1 for the uncertainty of the non-linearity.

(3) Spectral shape factor F_{SS}
This factor represents the uncertainties in the FRS caused by the variability in the base-isolated building. The 10% broadened FRS is used in the aseismic design of the RV. Therefore F_{SS} is defined by:

$$F_{SS}=\frac{(RV\,stress\ due\ to\ 10\%\ broadened\ FRS)}{(RV\,stress\ due\ to\ actual\ FRS)}=1.27$$

As mentioned in 4.2, the FRS has the variability shown in Fig. 5 and its COV is less than 0.3 for all input levels.
Therefore the enveloped value of 0.3 was used for β_R for simplicity although it overestimates the probability of RV failure at low input levels (e.g. $1.0 \times S_2$).

(4) Earthquake direction factor F_{EC}
This factor represents the earthquake component combination. The maximum stresses induced by horizontal and vertical forces are added in the design. It was assumed that the actual stress was the value estimated by SRSS and the summated value was a 95% confidence value. Therefore the factor is given by:

$$F_{EC} = \frac{(M/Z + F/A)}{\sqrt{(M/Z)^2 + (F/A)^2}}$$

The factor changes according to the input level since the ratio of the stresses depends on the input level. (See Table 1)

5.2 Capacity factors

(1) Strength factor F_s
This factor represents the ratio of the ultimate strength to the stress calculated in the design. The allowable stress σ_t in the design using the design yield stress and a factor of safety (F.S.) of 1.3 was 7.33 Kg/mm^2. Therefore the medium buckling strength σ_m was given by:

$$\sigma_m = \frac{\sigma_{y,mean}}{\sigma_{y,min}} \times F.S. = 1.3 \times 1.5 \times 7.33 = 14.3 \text{ Kg/mm}^2$$

On the other hand, the design stress is 4.9 Kg/mm^2. Therefore F_s was given by:

$$F_s = \frac{14.3}{4.9} = 2.92$$

Assuming $\sigma_{y,min}$ to be the 95% confidence value for $\sigma_{y,mean}$, β_R was given by:

$$\beta_R = \frac{\ln 1.3}{1.64} = 0.16$$

(2) Inelastic energy absorption factor F_μ
This factor represents the deamplification effect resulting from the inelastic energy absorption. Under repeated seismic loads, the nonlinear deformation produces a large damping effect in the seismic response. [3] Fig. 7 shows the actual seismic response including the damping is much less than the linear seismic response. The ratio $\ddot{X}_a / \ddot{X}e$ depends on the FRS at the RV floor level. In the $3.5 \times S_2$ case, the ratio was calculated by RV nonlinear analyses and the ratio was estimated to be 2.0. Therefore $F_\mu = 2.0$ and for the uncertainty in the RV nonlinear analyses.

5.3 Results

Table 2 summarizes the estimated safety factors. The safety factor F depends on the input level so that the medium ground acceleration capacity A changes as the input level increases. From the tendency shown in Fig. 4, the response of the RV was expected to increase drastically due to the hardening of the rubber bearings. Therefore F at $4 \times S_2$ was estimated to be 0.0 and was interpolated for a given PGA.
By substituting the values in the Eq. (2), the fragility curve shown in Fig. 8 was obtained.

5.4 Effects of the capacity of the RV and the isolation system on the fragilities

The following fragility analyses were made to evaluate the effect of the capacity of the RV and isolation system on the fragilities:

a. RV wall thickness: 35 mm increased to 50 mm

b. Rubber bearings: 750 ton decreased to 500 ton
(Rupture displacement : 68.9 cm increased to 103.4 cm)

The 95% confidence fragility curves are compared in Fig. 9. HCLPFs (High-Confidence,Low-Probability-of-Failure) and medium ground acceleration capacity in each case are summarized in Table 2.

6. DISCUSSION

The RV fragility has a sharply increasing shape because of the drastic increase in the RV response due to the hardening of the rubber bearings. From the curve for 95% non-exceedance probability, the HCLPF for RV buckling failure was estimated to be $2.6 \times S_2$ which implies sufficient seismic margin.
Comparing case 1 &2, 3&4, HCLPF were increased to some extent ($2.6 \times S_2$ to $3.1 \times S_2$) due to increasing the wall thickness of RV. However, A shows only a small change because the increased capacity is cancelled out by the drastic increase in the response of the RV due to hardening. On the other hand, comparing case 1 &3, 2&4, A was increased to some extent ($3.7 \times S_2$ to $4.2 \times S_2$) due to improving the capacity of the rubber bearings although the HCLPF shows a small change. Therefore it was concluded that the equipment fragilities in an isolated plant strongly depend on the hardening characteristics of the isolation system, i.e., the skeleton of the rubber bearings.
In other word, capacity of the equipment in a base-isolated building is generally between the initiation of the hardening and the rupture point of the rubber bearings irrespective of the strength of the equipment.

7. CONCLUSION

A fragility assessment based on response and capacity factors was carried out for a reactor vessel (RV) taking the non-linearity of the isolation system into account. The result shows that the skeleton of the rubber bearings is dominant in the failure probability and the shape of fragility curve irrespective of the strength of the equipment.

8. ACKNOWLEDGMENT

This study was carried out as a research project of Tokyo Electric Power Company, entitled "Seismic PSA for an FBR plant".

REFERENCES

1. Kato, M., Watanabe, Y., et al. 1995. Design study of the seismic-isolated reactor building of demonstration FBR plant in Japan. SMiRT-13, Vol.III: 579-584

2. R.P. KENNEDY and M.K. RAVINDRA 1984. Seismic fragilities for nuclear power plant risk studies. Nuclear Engineering and Design 79:47-68

3. Kawamoto,Y.,Sasaki,N., et al. Reduction of Seismic Responses of Shell Structures with Nonlinear Deformation Characteristics. SMiRT-11, Vol.E:257-262

Table 1 Safety factors for RV Buckling (Case: RV: 35 mm Rubber bearing:750 ton)

Safety Factor	Input level					β_R	β_U	
	S_2	2.25 $\times S_2$	2.75 $\times S_2$	3.5 $\times S_2$	4.0 $\times S_2$			
F_S	2.92					0.16	0.1	Stress margin for the ultimate strength
F_μ	2.0					0.0	0.1	Inelastic energy absorptionby RV
F_C	5.84					0.16	0.14	
F_{SS}	1.27					0.3	0.0	Uncertainty in FRS
F_D	1.0					0.0	0.1	Damping in RV
F_{SM}	1.0					0.0	0.1	Modeling of RV
F_{MC}	1.0					0.0	0.1	Modal combination
F_{EC}	1.22	1.30	1.35	1.39		0.2	0	Earthquake components
F_{ER}	1.55	1.65	1.71	1.77		0.36	0.17	
F_{SA}	1.0					0.3	0.0	Spectral shape of the input motion
F_M	1.0					0.0	0.1	Modeling of thebuilding
F_{NL}	1.0	0.96	0.92	0.57	0	0.0	0.1	Nonlinearity of the building response
F_{SR}	1.0	0.96	0.92	0.57		0.3	0.14	
F *1	9.05	9.25	9.19	5.89	0 *2	0.50	0.26	

*1 Interpolated values were computed at given input levels between the calculated input levels.

*2 F=0.0 at $4 \times S_2$ due to the drastic increase in the RV response before the rupture of the rubber bearings.

Table 2 Effects of changing RV strength and capacity of rubber bearings

Case	RV	Rubber bearing	HCLPF	A
1	35	750	2.6	3.7
2	50	750	3.1	3.8
3	35	500	2.6	4.2
4	50	500	3.5	4.3
	(mm)	(ton)	($\times S_2$)	($\times S_2$)

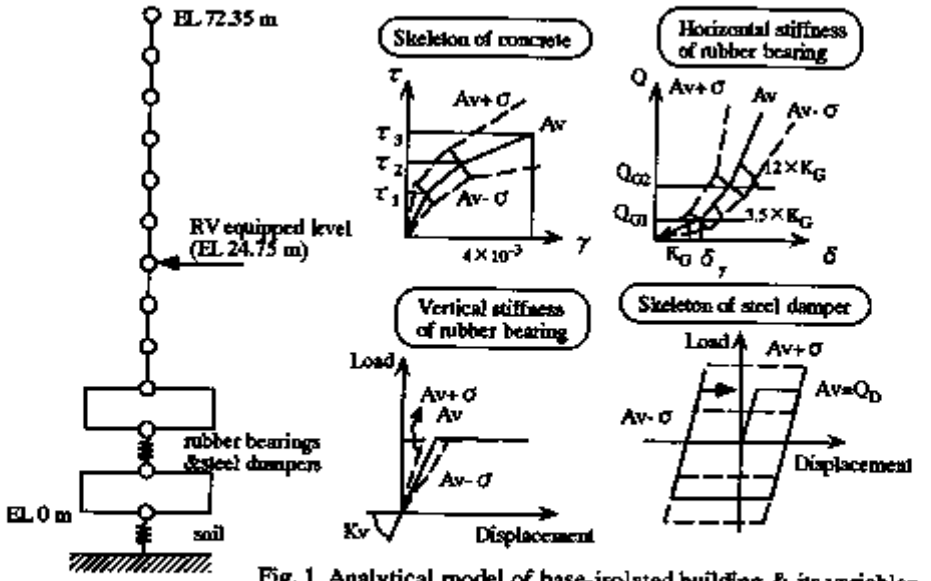

Fig. 1 Analytical model of base-isolated building & its variables

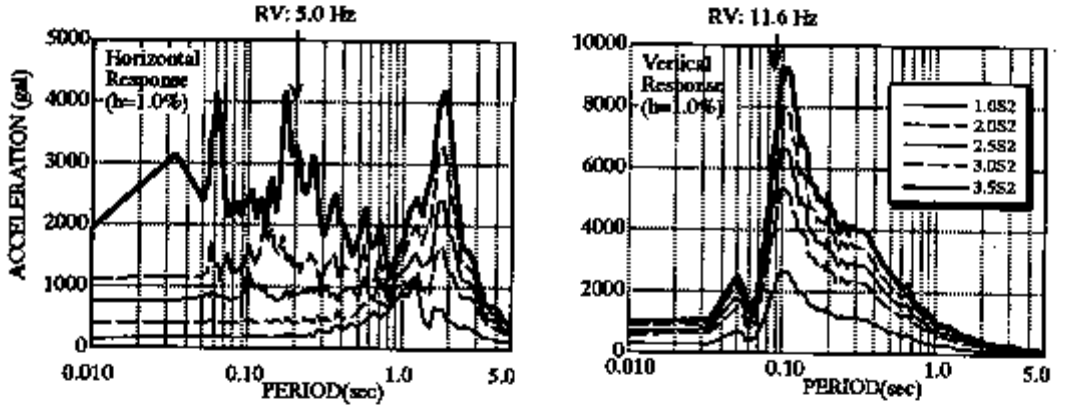

Fig. 2 Floor Response Spectra for various input levels

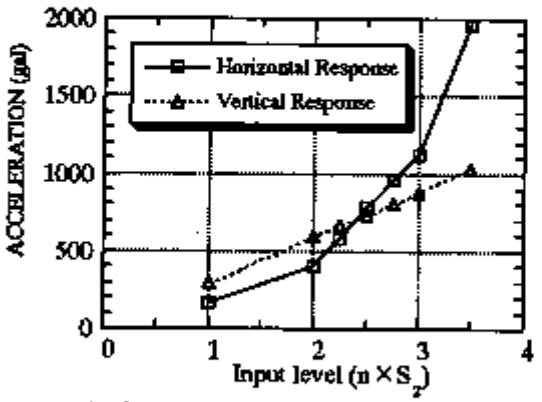

Fig. 3 Building response v.s. Input level

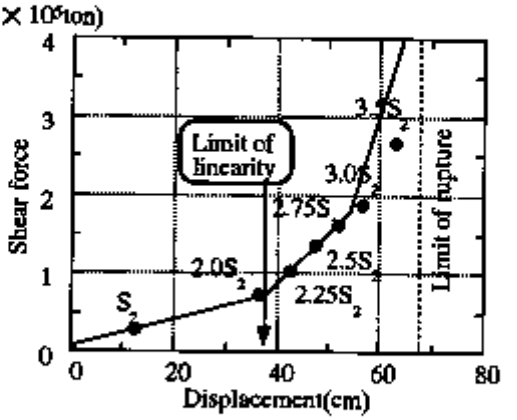

Fig. 4 Response of Isolation system v.s. Input level

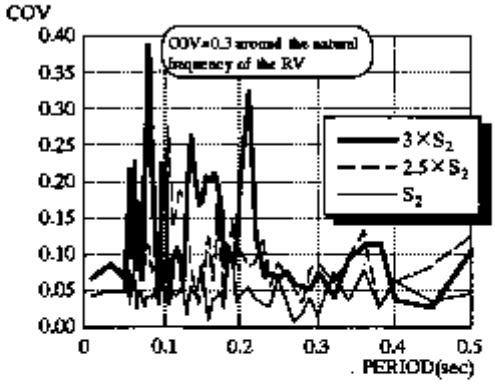

Fig.5 Response uncertainties due to the variability of the building

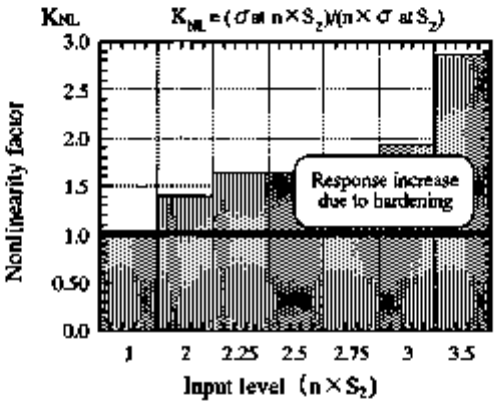

Fig. 6 Nonlinearity factor v.s. Input level

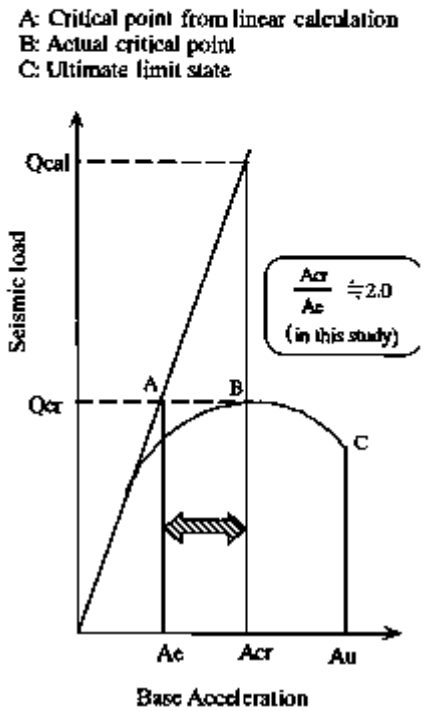

Fig. 7 Basic behavior of elasto-plastic buckling under seismic loads

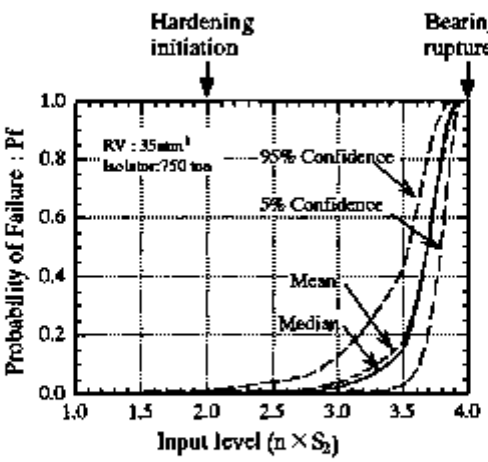

Fig.8 Fragility curve for RV backling

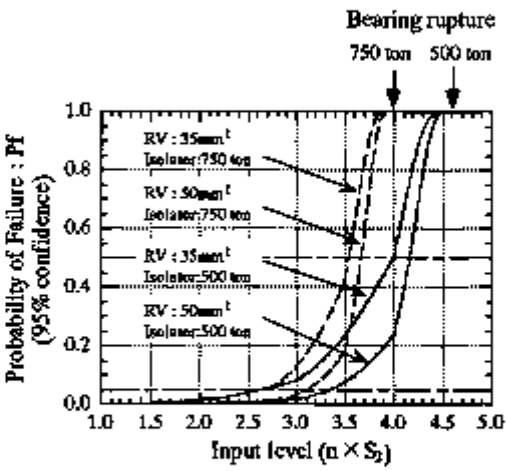

Fig.9 Effects of changing RV strength and capacity of rubber bearings

Transactions of the 14th International Conference on Structural Mechanics in Reactor Technology (SMiRT 14), Lyon, France, August 17-22, 1997 K11/6

Influence of soil properties on response of seismic base isolation of nuclear equipments

Ebisawa K.[1], Ando K.[1], Kameoka H.[2], Shibata K.[3]
(1) Japan Atomic Energy Research Institute, Japan
(2) CRC Research Institute, Inc., Japan
(3) Japan Atomic Energy Research Institute (JAERI), Japan

ABSTRACT: In order to investigate the influence of soil property on the performance of seismic base isolation for nuclear equipment, the response of emergency transformer without and with isolation devices is evaluated under the condition of the soil shear wave velocity (Vs) of range from 100 to 1500 m/sec. It was proved that the acceleration response of a component with devices is insensitive to the soil velocity except for Vs below 150 m/sec.

1 INTRODUCTION

Seismic base isolation of equipments is one of promising technique to reduce seismic risk of an existing or new plant. In order to establish design methodology of seismic base isolation of equipments, two studies have been carried out.

One is the study to develop a methodology for evaluating the effectiveness of seismic isolation of nuclear equipments. The methodology was developed by applying the theory of Reliability Engineering and the method used in seismic Probabilistic Safety Assessment (PSA) [1]. Based on this methodology, EBISA code has been developed [2]. An emergency transformer, which was identified to be an important equipment by previous seismic PSA [3], was selected for the case study of effectiveness evaluation by EBISA code. It was proved that the effectiveness can be influenced by the differences of the isolation devices and the direction of the input seismic wave [4]. In this study, however, an influence of soil property was not considered.

The another is the study to establish the design concept of seismic isolation of nuclear equipments. The equipments installed in various places both inside and outside the building were considered to be investigated. Thus various examinations corresponding to each installation condition are necessary. As for the equipments installed inside the building, it is important to evaluate the influence of building behavior on equipment response. From this viewpoint, the floor response in a BWR reactor building was studied [5].

On the other hand, as for the equipments outside the building, the influence of soil property on equipment response should be examined. In order to investigate the influence of soil property on the performance of seismic isolation for nuclear equipment, the above transformer was selected for the analysis. The influence of the shear wave velocity of soil property on the response of transformer with isolation devices was evaluated.

This paper describes the evaluation results of the influence of the soil shear wave velocity on the response of transformer with isolation devices.

2 METHODOLOGY FOR EVALUATING THE EFFECTIVENESS OF SEISMIC BASE ISOLATION OF NUCLEAR EQUIPMENTS

The procedure to evaluate the applicability and effectiveness of seismic isolation of equipments consists of two steps; quantitative and comparative evaluations, as shown in Fig.1.

In the first step, to decide the applicability of base isolated structures, the functional failure probability, $F(t)$, during the life time, t (year), of equipment without base isolation devices is quantified. In the case that $F(t)$ is significant in the context of safety and replacement cost considerations, the comparative evaluation is carried out. In the second step, the ratio of the functional failure frequency, λ (1/year), without base isolation devices to that with them is quantified. The effectiveness can then be judged based on the ratio as shown in Fig. 1.

$F(t)$ can be calculated according to the formula:

$$F(t) = 1 - \exp(-\lambda \cdot t). \tag{1}$$

Parameter λ can be calculated using the density function of seismic hazard [6], $H(\alpha)$, which represents the annual exceedance occurrence frequency of ground motion level above α, and the functional failure probability, $p(\alpha)$, of equipment under α as follows:

$$\lambda = \int_0^\infty \left[\left(-dH(\alpha)/d\alpha \right) \cdot p(\alpha) \right] d\alpha. \tag{2}$$

If the seismic response, $f_R(\alpha, x)$, that affects the equipment failure is independent of the seismic capacity, $f_C(x)$, of the equipment, $p(\alpha)$ can be expressed as follows:

$$p(\alpha) = \int_0^\infty f_R(\alpha, x) \left\{ \int_0^x f_C(x)\, dx \right\} dx, \tag{3}$$

where $f_R(\alpha, x)$ and $f_C(x)$ are the probability density function of the logarithmic normal distribution. x represents parameters of acceleration and stress etc. The $f_R(\alpha, x)$ is estimated based on the response factor method [7].

3 CONDITIONS OF RESPONSE ANALYSIS

3.1 Seismic Base Isolation Structure

(1) Structure of Transformer with Ceramic Tubes

The high voltage type emergency transformer of 275 kV consists of three ceramic tubes charged with the isolation oil, the body and the foundation etc. as shown in Fig. 2. The ceramic tube has a length of 3.22 meters, the maximum outside diameter is 490 millimeters. A weight of the ceramic tube and the body is about 1.9 and 78.1×10^3 kgf, respectively.

(2) Seismic Base Isolation Devices

The transformer is seismically isolated by the base isolation devices of a lead rubber bearing (LRB) type, which is suitable for heavy equipment such as the transformer. It is installed on each pedestal of square corners between the body and the foundation as shown in Fig. 2.

The bearing has a rated weight of 20×10^3 kgf, the horizontal stiffness corresponds to the natural period of 1.98 sec and the mean damping is about 20 %.

(3) Failure Mode of Transformer

The functional failure of the base isolation structure which consists of the transformer and isolation devices is supposed to be caused by at least one failure of the transformer and isolation devices. The vulnerable part of the transformer is assumed to be the area at the flange between tube and sleeve, and the functional failure mode was identified to be the leakage of isolation oil at least one tube based on the records of disaster earthquake [1].

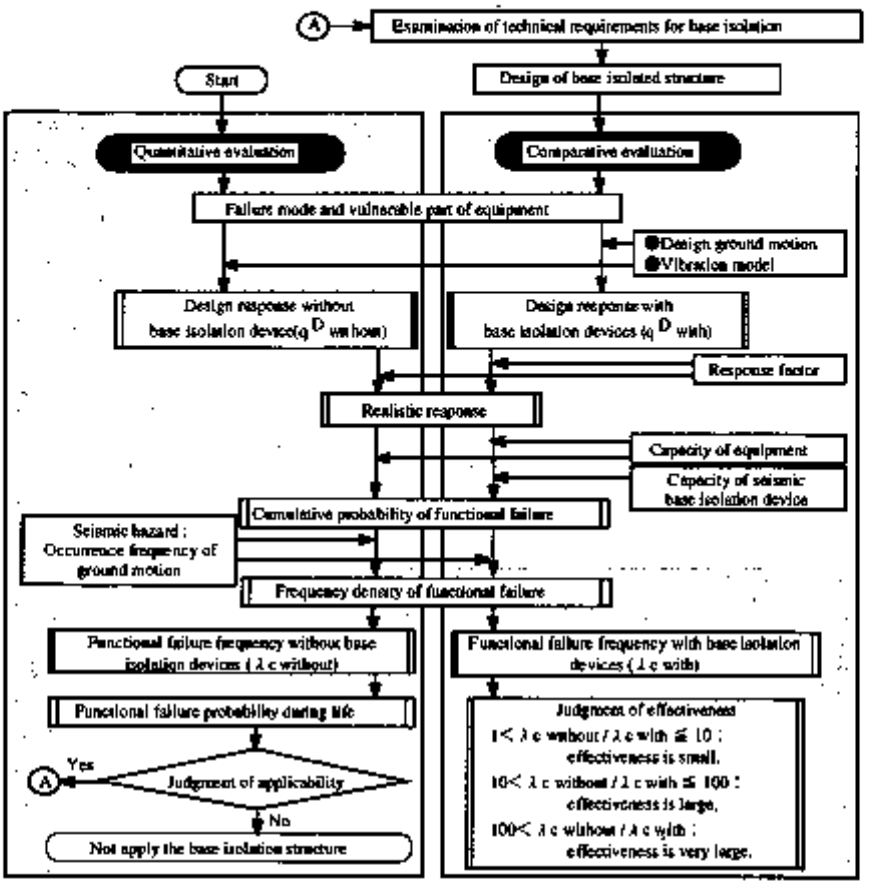

Fig.1 Evaluation methodology for applicability and effectiveness of seismic isolated structure

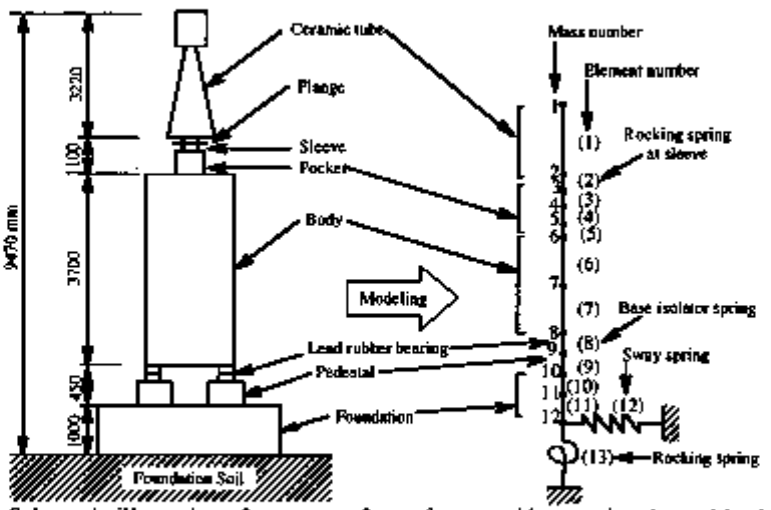

Fig.2 Schematic illustration of structure of transformer with ceramic tube and lead rubber bearing and multi-lumped mass vibration model

3.2 Response Analysis

(1) Procedure of Response Analysis

The responses of the transformer are calculated by the direct integration method using the time history of seismic motion and the multi-lumped mass vibration model as shown in Fig.2.

The main specification of the above vibration model can be described: The spring constants of sway and rocking, which represent the soil-transformer interaction, are estimated by the following Whitman and Richart theory [8] using the soil material values of the various shear wave velocities (Vs) of 100, 150, 300, 500, 1000 and 1500 m/sec.

$$K_S = 2(1+\nu)\cdot G\cdot \beta_x \cdot \sqrt{BL}, \qquad C_S = 0.576K_S \cdot R_S \cdot \sqrt{\frac{\gamma}{g\cdot G}}, \tag{4}$$

$$K_R = \frac{G}{1-\nu}\cdot \beta_\phi \cdot B\cdot L^2, \qquad C_R = \frac{0.30}{1+\beta_\phi}\cdot K_R \cdot R_R \cdot \sqrt{\frac{\gamma}{g\cdot G}}, \tag{5}$$

$$G = \frac{\gamma\cdot (V_S)^2}{g}, \tag{6}$$

where K_S and C_S are stiffness (kgf/cm) and damping coefficient (kgf・sec/cm) of sway spring, K_R and C_R stiffness (kgf・cm/rad) and damping coefficient (kgf・cm・sec/rad) of rocking spring, and G shear modulus (kgf/cm^2). The nomenclature and values of the others parameters in the above equations are shown in Table 1. The spring constants of sway and rocking corresponding to each value of the above shear wave velocity are shown in Table 2.

The sway spring constant of LRB is 5.1×10^2kgf/cm. The rocking spring constant between the sleeve and the ceramic tube is based on data of the Society of Electrical Co-operative Research and has a value of 1.0×10^8 kgf・cm / rad [9].

Table 1 Nomenclature and Values of Each Parameter in Evaluation Equations of Sway and Rocking Constants

γ	Density of Soil	2.1×10^{-3}(kgf/cm^3)	R_S	Equivalent Radius of Foundation for Sway Spring	691(cm)
ν	Poisson's Ratio of Soil	0.438	R_R	Equivalent Radius of Foundation for Rocking Spring	2764(cm)
g	Acceleration of Gravity	980(cm/sec^2)	β_x	Correct Constant of Sway Spring depending on Ratio of L/B	1.1
B	Width of Foundation	1500(cm)	ν_ϕ	Correct Constant of Rocking Spring depending on Ratio of L/B	0.46
L	Length of Foundation	1000(cm)			

Table 2 Evaluation Results of Shear Modulus, Sway and Rocking Spring Constants of Soil

		Shear Wave Velocity Vs (m/sec)					
		100	150	300	500	1000	1500
Sway	Stiffness $K_S\times10^5$ (kgf/cm)	8.3	18.7	74.7	207.5	830.0	1867.5
	Damping Coefficient $C_S\times10^3$ (kgf・sec/cm)	33.0	49.6	99.1	165.2	330.0	495.5
Rocking	Stiffness $K_R\times10^{11}$ (kgf・cm/rad)	2.6	5.9	23.7	65.7	262.9	591.4
	Damping Coefficient $C_R\times10^9$ (kgf・cm・sec/rad)	20.3	30.4	60.8	101.3	202.5	303.8
Shear Modulus $G\times10^2$ (kgf/cm^2)		2.1	4.8	19.3	53.6	214.3	482.1

(2) Input Seismic motions

Seismic motions, S_1F and S_1N, with different characteristics are chosen on input data. They are obtained from the maximum design earthquake in accordance with the Regulatory Guide [10] and used as the design basis ground motions for the structures and equipments of Japanese nuclear power plants.

S_1F has the predominant frequency of about 2.7 Hz, and the maximum acceleration of 287 Gal. S_1N has that of about 6.7 Hz, and 267 Gal.

These acceleration response spectra are shown in Fig. 3.

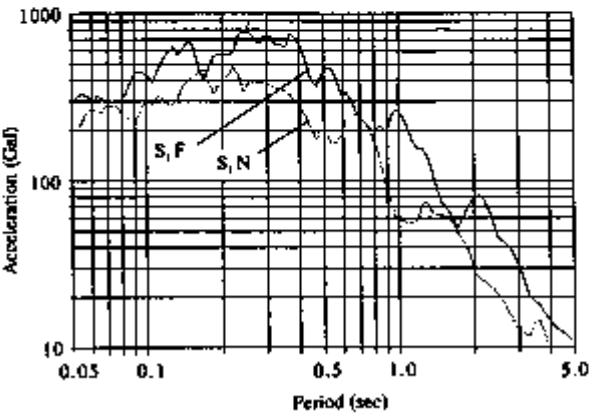

Fig.3 Acceleration Response Spectra of S_1F and S_1N

4 RESULTS OF RESPONSE ANALYSES

4.1 Natural Period of Transformer without and with Isolation Devices

The natural periods of the transformer without and with isolation devices under Vs range from 100 to 1500 m/sec are shown in Table 3.

From Table 3, the primary period of transformer without devices depends on the rocking of the ceramic tube and is the almost constant value of 0.15 and/or .013 sec. The secondary period depends on the sway of the foundation which represents the soil-transformer foundation interaction, and decreases gradually and settles down to the almost constant level of 0.02 sec with an increase of Vs. The primary and secondary periods at Vs of 100 m/sec are similar.

On the other hand, the primary and secondary periods of transformer with devices are 1.98 sec by the sway of the isolation devices and 0.14 sec by the rocking of the ceramic tube, respectively and are almost similar value for the range of Vs examined.

Table 3 Natural period of Transformer without and with Isolation Devices

Natural Period		Shear Wave Velocity of Soil Vs (m/sec)						Remarks
		100	150	300	500	1000	1500	
Without Isolation Devices	Primary (sec)	0.15	0.13	0.13	0.13	0.13	0.13	Rocking of Ceramic Tube
	Secondary (sec)	0.13	0.10	0.05	0.03	0.02	0.02	Sway of Foundation
With Isolation Devices	Primary (sec)	1.98	1.98	1.98	1.98	1.98	1.98	Sway of Isolation Devices
	Secondary (sec)	0.14	0.14	0.14	0.14	0.14	0.14	Rocking of Ceramic Tube

4.2 Responses of Transformer without Isolation Devices

The acceleration at the ceramic tube without isolation devices to S_1F and S_1N are calculated under Vs range from 100 to 1500 m/sec.

Fig.4 shows the acceleration response time histories at the ceramic tube at Vs of 100 and 1500 m/sec to S_1F. The maximum accelerations are about 1024 and 702 Gal, respectively. Fig.5 shows the relationship between the maximum acceleration and Vs to S_1F and S_1N.
As shown in Fig.5, the responses of transformer are very high at Vs of 100 m/sec, while it decreases steeply and settles to the almost constant level with an increase of Vs.

Under the response analysis conditions of this paper, the sway and rocking stiffness are considered to be soft in Vs range below 150 m/sec and to be rigid over 150 m/sec. Thus the influence of the soil property on the responses of transformer is large at Vs range below 150 m/sec but not over 150 m/sec.

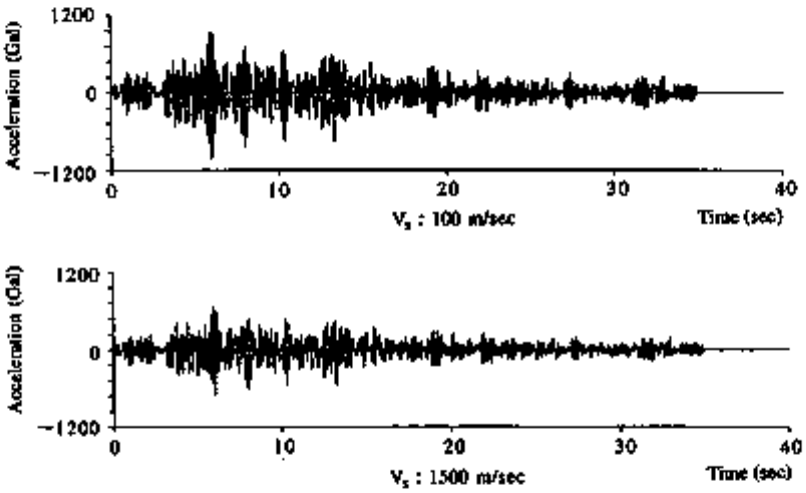

Fig.4 Acceleration Response Time Histories at the Ceramic Tube at Vs of 100 and 1500 m/sec to S_1F

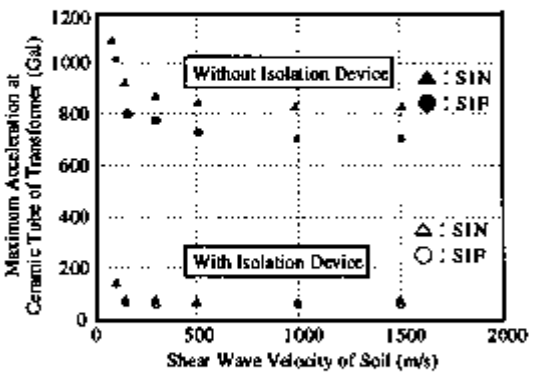

Fig.5 Relationship between Maximum Acceleration of Ceramic Tube and Shear Wave Velocity of Soil

4.3 Responses of Transformer with Isolation Devices

The acceleration responses of the transformer with isolation devices to S_1F and S_1N are calculated under the same condition as that without devices. The acceleration response time histories at the ceramic tube and the transformer body at Vs of 100 and 1500 m/sec to S_1F are shown in Fig.6 and Fig.7, respectively. The relationships between the maximum accelerationof the ceramic tube part and Vs to S_1F and S_1N are also shown in Fig.5.

The acceleration time histories of the transformer body as shown in Fig.6 and Fig.7 are dominated by the isolation devices that have natural period of 1.98 sec. On the other hand, it is shown that the time histories of the ceramic tube having that of 0.14 sec are superposed on that of the body.

From Fig.5, it is found that the acceleration responses of the transformer with devices are much smaller than that without devices and the acceleration values are almost constant for the range of Vs examined except for Vs below 150 m/sec.

These results indicate that the acceleration of a component with isolation devices is insensitive to the soil velocity except for Vs below 150 m/sec, since the stiffness of isolation devices are much smaller than that of soil.

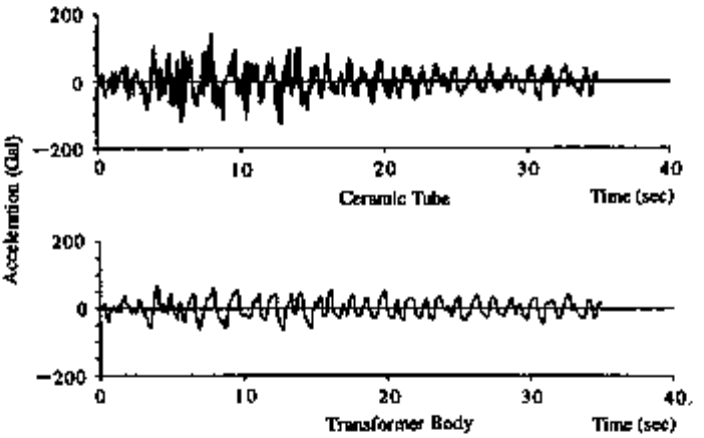

Fig.6 Acceleration Response Time Histories at Vs of 100 m/sec to S_1F

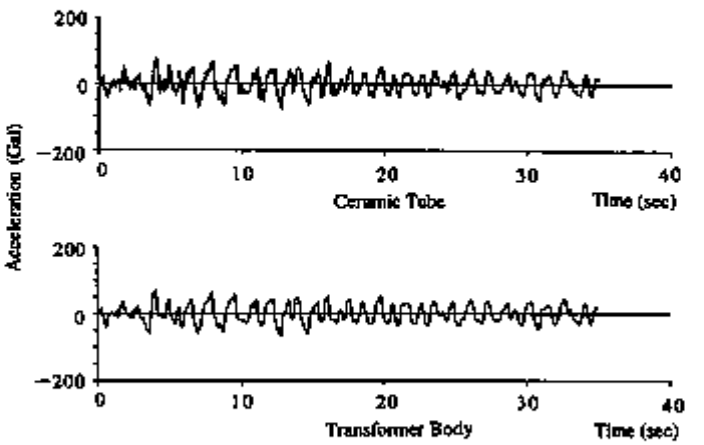

Fig.7 Acceleration Response Time Histories at Vs of 1500 m/sec to S_1F

5 SUMMARY

In this paper, it is indicated that the acceleration of a component with the isolation devices is insensitive to the soil velocity except for Vs below 150 m/sec.
Thus the shear wave velocity of soil is not important parameter except for Vs below 150 m/sec and its influence on the acceleration of a component outside the building may be ignored in the seismic base isolation design except for the above Vs range.

References

[1] K.Ebisawa and T.Uga: Evaluation methodology for seismic base isolation of nuclear equipments, *Nucl. Engrg. and Des.* 142, 1993.

[2] K.Ebisawa : Evaluation methodology for seismic base isolation of nuclear equipments and evaluation code EBISA, *RIST NEWS*, No.20, 1995. *

[3] NRC: *NUREG-1150*, ,1989.

[4] K.Ebisawa, et al.: Influence of various parameters on effectiveness of seismic base isolation of nuclear equipments, *SMiRT 13*, KB08, 1995.

[5] K.Ebisawa, et al.: Methodology for estimating realistic response of buildings and components under earthquake motion and its application, *Japan Atomic Energy Research Institute-Research* 96-059, 1996.*.

[6] K.Ebisawa, et al.: A methodology of probabilistic seismic hazard evaluation and sensitivity study, *Journal of Japan Society of Civil Engineers*, Vol.437/I-17, 1991.*

[7] K.Ebisawa, et al.: Evaluation of response factors for seismic probabilistic safety assessment of nuclear power plants, *Nucl. Engrg. and Des.*147, 1994.

[8] Whitman, R.V. and Richart, F.E.: Design procedures for dynamically loaded foundations, *J. of Soil Mech. and Fond. Div. ASCE*, Vol. 93, No. SM6, 1967.

[9] Society of Electrical Co-operative Research: Seismic design of transformer with ceramic isolator, *Electrical Co-operative Report*, Vol.38, No.2, 1982.*

[10] Nuclear Safety Commission, Japan: *Examination guide for seismic design of nuclear power reactor faculties*, 1981.

*: In Japanese

Transactions of the 14th International Conference on Structural Mechanics in Reactor Technology (SMiRT 14), Lyon, France, August 17-22, 1997 K12/3

New method of bench dynamic testings of NPP seismic isolation systems and equipment

Bellayev V.S., Vinogradov V.V., Sirro V.A.
Scientific Research Center, Russia

ABSTRACT: Development of seismic explosive tables for testing NPP large-sized objects are being continued in Russia. Seismic explosive technology for seismic testings permits to enhance essentially the capabilities of reprodicing the parameters of destructive earthquake effects, especially for high building marks comparing with motor-driven seismic platforms.

1. MAIN PRINCIPLES OF SEISMIC EXPLOSIVE TECHNOLOGY FOR THE SEISMIC TESTINGS.

Within the recent years the problems of experimental check of operation and stability evaluation of diverse NPP objects and their elements (structures, building constructions, systems, components etc.) under the conditions of destructive-earthquake-type effects have assumed great importance. On the complex of ground shake tables (these tables are under operation in Russia for more than 20 years) the reproduction of the dynamic loads, caused by such effects, is realized using the explosive technology. The complex incorporates a set of stands with load-carrying capacity up to 300 tons, the largest seismic platform dimensions make up 30 x 12 m. According to the technology developed such reproduction of the necessary loading conditions of the objects under study is carried out due to

energy effect of firing the explosive charges on the bearing structures of the test stands and further transformation of the kinematic processes with the help of special forming devices. In order to set the necessary direction of the test stand structures movement the explosive charges firing can be carried out both in the soil (directly under the test stand or on the side of it), and in the special load actuators, which are installed on the test stand and creat jet power (recoil force). As forming devices for transformation of the test stand kinematic processes to the required test parameters the elements of various type and design (pneumatic, hydraulic, pneumo-hydraulic, mechanical etc) are used. Chosing the weight and the quantity of the explosive charges, conditions of their arrangement (placement distance and depth, installation in the actuators, etc), setting the firing sequence, as well as application of the forming devices with certain characteristics, changing the devices layout and operation mode etc. ensure forming the loads of the required type, rate and frequency content.

2. ADVANCEMENT OF THE SEISMIC EXPLOSIVE TECHNOLOGY METHODS.

In 1995 the complex was incorporated with the CC500/300 test stand, designed for testing the structures (seismic isolated structures included) and the equipment of various designation. This stand includes a rectangular steel fragment of a building with dimension 22 x 6 x 7 m and weight 400 tons, supported with the help of the removable support elements or the seismic isolators on the movable supports. Fig. 1 presents a schematic diagram of the test stand CC500/300. Simulation of seismic vibrations, which are similar to the earthquakes effects, is produced with the help of two forming cascades. The first of them includes two support platforms (rigid steel beam structures), which are installed on the base slabs with the help of the rollers. With the help of lateral forming pneumatic elements, located on the ends, and fixing (hammer) device the support platforms

move in the horizontal direction. The first test stand cascade introduces to the system the major low-frequency component within the range between 1 and 2.5 Hz. The second cascade consists of two intermediate platforms which include bearing areas for the test stand table supports. They are located above the first forming cascade on the pneumatic elements. Energy input to the system is provided by application of the powder load actuators which are installed in pairs on the sides of the intermediate platforms. Attachment of the actuators provides for the capability to change the slope angle to control the vertical and horizontal movement component.

The Ir pulse, obtained from the powder load actuators, is calculated according to the following dependences:

$$Ir = \int_0^{tu} Qr(t) \cdot dt \qquad (1)$$

where tu - pulse time;

$$Qr(t) = Pr(t) \cdot Sr,$$

here Pr(t) - pressure of gases, acting on the working medium;
Sr - cross sectional area of the actuator barrel;

$$Pr(t) = \begin{cases} 0 & , \text{ at } t=t0=0; \\ Prmax \cdot t/tn & , \text{ at } t<tn; \\ Prmax \cdot (hk/(hk+Zb))^j & , \text{ at } tn<t<tb; \\ Prmax \cdot (hk/(hk+htp))^j \cdot (tu-t)/(tu-tb), & \text{ at } tn<t<tb; \end{cases} \qquad (2)$$

where hk - length of the explosive chamber;
htp - length of the actuator operating compartment;
j - adiabatic curve index;

$$Prmax = 125.5 \cdot \nabla^{0.753}, \text{ [kPa]}$$

$$\nabla = wr/wk, \text{ [kPa]}$$

here wr - weight of the powder charge;
wk - initial volume of the explosive chamber.

The second cascade forms, mainly, the vibrations within the range between 2 and 5 Hz. On four support units of the

shock-absorbers, suported on the areas of the second forming cascade a two-storied building fragment which represents a test stand table is installed.

Changing the parameters of firing, reaction time, angle of inclination of the powder load actuator, value of the initial pressure in the vertical and lateral pneumoelements, on the intermediate platforms of the second forming cascade there are created non-stationary effects, equivalent to the earthquake loadings of severe earthquakes, with the required frequency content in the preset amplutude time domain. The type of characteristic test effect, formed by the stand, is shown on the Fig.2.

The test stand is designed for the following problems solution:

- testings of large-sized objects with the weight up to 500 tons, installed directly on the intermediate platforms. Testings objects with the weight up to 300 tons can also be placed on the first, second storey and the roof of the building fragment.
- integrated testings of the actual seismic isolation systems or their fragments with load-carrying capacity up to 500 tons. On the intermediate platforms of the second forming cascade there are provided positions for installation of the seismic isolation and damping devices. The test stand table structure gives the opportunity to reproduce both the changes of kinematic parameters on the various marks of the isolated object and their effect on the equipment.

3. METHODICAL BASES OF THE SEISMIC TESTINGS OF NPP SEISMIC ISOLATION SYSTEMS.

On the each unit of the seismic explosive stands complex there is ensured realization of three main test modes:

- "seismic shock" mode reproduces vibrations of the building constructions and equipment attachment units at the inputs, for example, of near industrial explosions;
- "rigid seismic" mode simulates, among the other things,

seismic vibrationson the high (12.0 m and higher) marks of buildings and structures, as well as model loads in accordance with the similarity laws;

- "soft seismic" mode simulates the ground motion and the motion of the building foundations under the conditions of various earthquake rates.

In this case the support blocks motion of the object under study in accordance with the testings purposes has a form of spatial, flat or one-dimensional non-stationary vibrations. Limits of the changes in the characteristic peak values of the loadings in the area of [0;200 Hz] frequencies are presented in the Table 1.

Table 1

Type of loading mode	Acceleration (g) along the axes		Velocities (m/c) along the axes		Displacements (m) along the axes		Durations of the load input, c
	oz	ox(oy)	oz	ox(oy)	oz	ox(oy)	
shock-seismic	+30/ -10	40	+3/ -1	3	+0.5/ -0.2	0.5	to 1.0
rigid-seismic	10	10	2	2	0.5	0.5	to 5.0
soft-seismic	2	2	1	1	0.7	1.0	to 30.0

Thus far in the world practice a considerable volume of data on the seismic isolators simulation tests has been accumulated. In this circumstances a transfer to full-scale experiments with seismic isolators and, especially, with the fragments of NPP buildings seismic isolation systems is of special interest. Specifications of the seismic explosive stands complex ensure the opportunity to provide such seismic full-scale testings under the conditions of "soft seismic" (see table) mode. The technique of preparing and testing the the elements and fragments of the NPP full-scale seismic isolation systems provides for a series of measures, the basic of which are:

- development of technology of erection, starting-up and adjustment and repair jobs under the near-service conditions;

- determination of the seismic isolation facilities operability;
- determination of the dynamic efficiency of the seismic isolation facilities for the real operation conditions.

Development of erection and and adjustment technology of the shock seismic protection facilities on the test beds permits to improve the technological tools for execution of such operations under the real operation conditions. In each particular case the technology will be determined by the clearances for the transportation and erection areas of the seismic protection facility elements on the object, by the opportunity to use the lifting devices, by the sequence of operations etc. The test stand base presents unique opportunities for simulation and development of the erection technology.

Determination of operability and efficiency of the seismic isolation facilities includes a set of investigations of both the separate elements and a fragment of the system for various operation conditions. Such operations shall include the testings of single seismic isolation facilities on the various static loads, impacts, parameters of the seismic isolators characteristics (preasure, initial height, damping property etc), kinematic parameters (maximum deformation and deformation rate) under various temperature condition. Realization of the testings on the test stands is carried out by way of fixing one side of the test platform to the stand body with the help of cylindrical or ball hinges. Under the center position of the opposite side a seismic isolator to be tested is installed, and the platform is loaded in this position with ballast weights up to the required force in the shock-absorber. Explosive charges under the stand body or on the side of it actuate the platform, causing the seismic isolator deformation in the necessary direction.

The most complicated and labour-consuming are the testings of a fragment of the seismic isolation system. The total scope of the modes to be tried-out for all operation conditions and occurrence of possible emergency situations shall provide for the following seismic testings conditions.

1. Testings on the earthquake-equivalent effects, specified by the response spectra (standard spectra, spectra of specific accelerogramms for the object siting area, integrated spectra for the accelerogramm set).
2. Testings having regard to the azimuth and (or) angular rotations of a seismic isolated structure, induced either by the time delay in the waves arrival to the support seismic isolator elements, or caused by the initial angular rotations of the seismic isolated structure because of the base slab inclination or nonuniform permanent deformation of the supports.
3. Testings on the equivalent effects which are different because of the angular motion of the support foundation or due to different modes of motion of the foundation points in the positions of the seismic isolators placement.
4. Initiation of a motion with required or maximum conceivable deformations and rates of the seismic isolators and damping devices deformation. Such test conditions would be required also when checking the influence of the attached cable and engineering communications on the protected object motion and when checking their structural behaviour.
5. Testing of the seismic isolation systems when the seismic isolators specifications depart from the rated ones due to long-term operation, partial loss of tightness, slipping or partial destruction of the connections, caused by previous earthquake, etc.
6. Testings of the seismic isolated structure at the system centre of mass eccentricity (preset or appeared while in service) for the conditions of non-adjusted position of the structure or during the recovery of its setting position due to redistribution of forces in the seismic isolators.

4. CONCLUSION.

This approach is realized during the testings with the help of the seismic explosive stands of the full-scale fragment of multicomponent low-frequency seismic isolation of the NPP reactor building with VVER-640. Testing is to be completed in 1997.

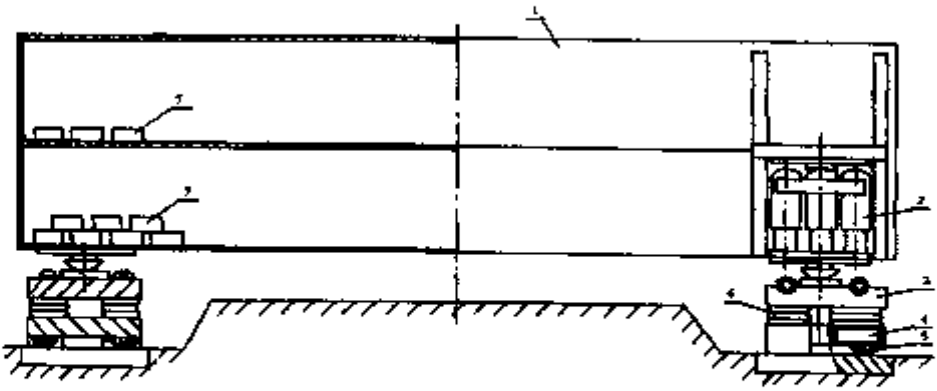

1 - testing construction (fragment of a building)
2 - support elements
3 - movable supports
4 - support platforms
5 - rollers
6 - pneumatic elements
7 - testing equipment

Fig. 1. Shematic diagram of the test stand.

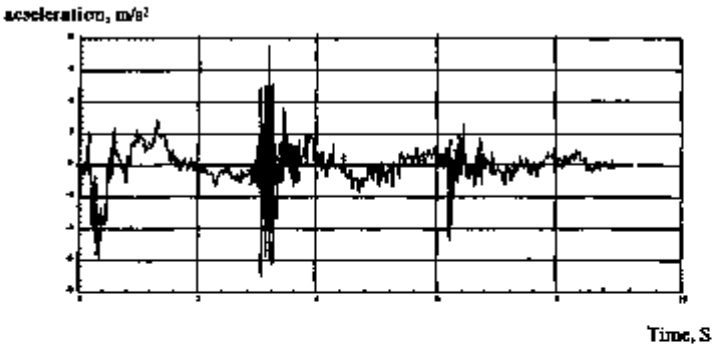

Fig. 2. The process of the stand motion.

Transactions of the 14th International Conference on Structural Mechanics in Reactor Technology (SMiRT 14), Lyon, France, August 17-22, 1997 K11/5

Response analyses considering uncertainties of structural characteristics for base-isolated reactor building

Kato A.[1], Somaki T.[2], Shirahama K.[2], Hirotani T.[3]
(1) The Japan Atomic Power Company, Japan
(2) Obayashi Corporation, Japan
(3) Shimizu Corporation, Japan

ABSTRACT : Seismic response analyses for the base-isolated reactor building were conducted with considering uncertainties of structural characteristics. This paper describes the results of two examinations, which were quantitatively to evaluate the influence degree of such uncertainties on the response in the case of the design of the above building and to estimate the seismic safety margin against the design earthquake through the reliable probability approach. Further, these analyses were conducted based on the Monte Carlo simulation technique.

1. INTRODUCTION

It is necessary to grasp the variability of the building response resulting from the possible uncertainties in the material properties of the structure, soil and so on in the case of the design of the base-isolated reactor building. The objectives of this paper are the followings;

- It is to investigate what factor in structural characteristics should be especially considered in the design of the base-isolated reactor building and the equipment included in such a building
- It is to investigate that the base-isolated building secures the enough seismic safety margin as well as the seismic designed building from the viewpoints of failure probability assessment.

Two studies as shown under were conducted;

1) Horizontal seismic response analyses and vertical ones to evaluate the influence of such uncertainties on the building response and the floor response spectra for the design earthquake.
2) Fragility analyses to estimate the seismic safety margin from the viewpoint of probability.

These analyses were conducted based on the Monte Carlo simulation technique with the variability of those selected factors considered(Sample:100).

2. INFLUENCE DEGREE ON RESPONSE

2.1 Estimation of uncertainty for the design factor

The uncertainty of the possible design factor that have an influence on the response of base-isolated building was investigated and its value is estimated on the basis of past experimental results or analytical studies.

The analytical models were made based on base-isolated Fast Breeder Reactor (FBR) building designed in Japan[1]. The models are single-stick lumped mass model considering

both isolation layer and soil-structure interaction as spring. The design specifications of base-isolation system are shown in Table 1 and Fig. 1. respectively. The combination of natural rubber bearing and steel damper were used for base-isolation system as representative. The uncertainty of input-motion is not considered in this section.

The factor was arranged in terms of the parts of analytical model; soil spring, rubber bearing, steel damper and building.

The uncertainty of soil spring was represented in that of the shear wave velocity Vs. The value of uncertainty for Vs was estimated as 0.10 in the coefficient of variation (abbreviated as COV). Stiffness and damping coefficient of soil spring (horizontal, rotational and vertical) were set as proportional to the square of Vs and Vs itself, respectively.

In the case of the rubber bearing (abbreviated as Isolator), horizontal and vertical stiffness were considered. The uncertainty was evaluated based on accepting tests of actual building. The COV of horizontal and vertical stiffness were estimated as 0.05 and 0.10, severally, and were set as independent each other. The rotational stiffness was set as proportional to the vertical one.

The uncertainty of characteristics of steel damper was represented by that of material. The COV of the stiffness and yield strength were estimated as 0.03 and 0.10, respectively.

The design strength of concrete Fc was considered to be the representative for the design factor of building. The COV of Fc is evaluated as 0.13. Shear stiffness and axial stiffness of building were set as proportional to square root of Fc.

2.2 Uncertainty of response and effective design factor

The preliminary studies evaluating the sensitivity of each design factor were done by considering the variety of each factor one by one. Design factors that have great influence on horizontal and vertical response results are selected as shown in left part of Table 2 and Table 3, respectively. In the case of horizontal response, all characteristics of soil spring and the rotational spring of isolation system were neglected since their influence were very little.

By considering the uncertainties of selected design factors, horizontal and vertical response analyses were performed as follows.

(1) Make 100 samples of each factor according to the normal distribution by using the design value (as mean value) and COV.

(2) Carry out the response analysis using these samples of all factors in random order. Evaluate the uncertainties of response value from this case, named "All Variable".

(3) Carry out the response analysis considering one factor as fix, while the other factors are varied. Evaluate the influence of each design factor comparing these results each other or with that of (2).

Table 2 and Table 3 show analysis cases. The extreme design earthquake S_2-D[1] with maximum accelerations of 380 cm/sec^2 is used as input wave.

Following three response values were evaluated and analyzed statistically; horizontal displacement of bearing, horizontal and vertical floor response spectra (FRS) at the support point of the reactor vessel (h=0.01).

Fig. 2 shows the example of FRS in the case of vertical "All Variable". The FRS was represented by Rmax; maximum value in effective range for equipment as shown in Fig. 3.

Fig. 4 shows the distributions of horizontal displacement of isolator. It varies around 0.07 for COV. It is confirmed that the strength of steel damper has a great influence, though the other design factors such as the stiffness of rubber bearing have small influence..

Fig. 5 shows the distributions of vertical FRS represented by the Rmax. It varies around 0.1 for COV. The shear wave velocity of soil Vs shows dominant effect, while other design factors affect little.

In the case of horizontal FRS, the design strength of concrete Fc has the greatest influence and the stiffness of steel damper has smaller. The effect of other factors is negligible..

3. FRAGILITY ASSESSMENT

3.1 Procedure

The seismic safety margin of the base-isolated building against the design earthquake was estimated through the reliable probability approach.

The object of the building and the variability of structural characteristics were the same as the above, but the non-linear characteristics of the superstructure, isolators and the soil were additionally considered in the analytical model.

Fig. 6 shows the variability of the skeleton curve (structural characteristics). The mean of the skeleton curve was the design value, but the mean for the shear walls was evaluated assuming that the concrete strength Fc was 1.5 times the design value based on the actual building. The variability were considered in G, τ_1, τ_2, τ_3, γ_1, γ_2 and γ_3 for shear walls, K_{dt} and γ_{cu} for isolators, K_D and Q_D for dampers, where ,as for G, τ_1 and τ_3, the randomness due to themselves based on test results were considered in addition to that due to the design estimation by the variable Fc. The mark of shade and white in Fig. 6 signify the independence and the dependence on another factor, respectively.

The design input earthquake was changed to the imaginary earthquake S_2[2] with the velocity of 200kine in the relatively long period contents and the maximum acceleration of 830cm/sec^2 (PGA), which is considered to be the greatest earthquake in Japan.

As for the design specification of isolation system, the yield coefficient β of 0.05 was changed to 0.10. But the isolated natural period T_1 and T_2 were the same as the above study. The combination of natural rubber bearing and steel damper was considered for the isolation device.

The response variability βs, which was employed in fragility assessment, was evaluated through the non-linear seismic response analyses with the amplified earthquake S_2. The variability βu due to the uncertainty (see Table 4) was evaluated as the analytical error by comparison between the response analyses and the shaking table test results[3].

3.2 Results

Fig. 7 shows the response results of the typical members (shear wall of 1st-story and isolation layer). Fig. 8 shows the mean and standard deviation of such results by relationship with PGA.

The response of shear wall increased like the square curve of PGA, but the one of the isolation layer increased almost linearly(see Fig. 8). The COV of shear walls fluctuated due to the degree of the non-linearity, but the COV of the isolation layer was almost constant. In this paper, the response variability βs was estimated from the results at $2.5S_2$ input level with engineering judgment, since the collapse of shear walls and rupture of isolators occurred at $2.5S_2$ input level.

As for the responses at the support point of the Reactor Vessel, the maximum response acceleration(ZPA) increased like the square curve of PGA, as shown in Fig. 9(a). But the variability increased gradually in proportion to PGA (see Fig. 9(b)).

The probability of failure was calculated by the expression as shown in footnotes of Table 4, where the relationships between the mean of response(S) in each member and the input level(PGA) was evaluated due to the regression analysis. Table 4 shows the results of the fragility assessment of base-isolated reactor building.

Fig. 10 shows the fragility curves with estimated by 95% confidence for all members. Probability of failure for this building was estimated to be $Pf=1.38\times10^{-9}$, where that of the isolation layer was the greatest. From the viewpoint of the reliability based design, the allowable probability of failure in the Western countries is shown to be $Pfa=10^{-5}$-10^{-7} as a tentative proposal for the concrete containment vessel, which is the most important structure in nuclear power plant facilities[4]. As the above Pf was much less than this proposal

notwithstanding that the results of hazard analysis were not considered, it was confirmed that this building has the enough seismic safety margin.

In this connection, the value of the High Confidence Low Probability of Failure(HCLPF), which is alternative safety standard, was 1390cm/sec^2 (1.67S_2).

4. CONCLUSION

It was verified that the uncertainty of the yielding strength of damper has a tremendous influence on the response displacement of the isolator, which is considered to be an index as the seismic safety margin, though the uncertainty of the stiffness of the isolator has a little influence.

As for the horizontal response spectra at the support point of the R/V, the COV was calculated to be 5% to 10%, which was considered not effective to the design of equipment. On the other, the COV of vertical response spectra at the same point was calculated to be 10%, wherefore the uncertainty of the stiffness of the soil has the greatest influence on it.

From the result of the fragility analyses, which were conditioned that the input earthquake S_2 used was only the greatest tentative earthquake in Japan, the probability of failure assessment at wave S_2 level for the components (shear walls or isolators) of the base-isolated reactor building were lower than the order of E-8. Therefore it was verified that the base-isolated reactor building secured enough the seismic safety margin for the earthquake.

5. ACKNOWLEDGMENT

This study is carried out as a part of the FBR common research of the electric power companies in Japan, entitled "Technical Study on Optimization of Isolated FBR Plant (Part 2)".

REFERENCES

1. Kato, M., Watanabe, Y., et al. 1995. Design study of the seismic-isolated reactor building of demonstration FBR plant in Japan. SMiRT-13, Vol.III: 579-584
2. Kato, M., Watanabe, Y., et al. 1993. Study on ultimate behavior of base isolated reactor building. SMiRT-12, Vol.K2: 315-320
3. Kato, M., Watanabe, Y., et al. 1993. Multi directional earthquake input test and simulation analysis of base isolated structure. SMiRT-12, Vol.K2: 237-242
4. Hwang, H. et. al. 1985. Probability Based Load Combination Criteria for Design of Concrete Containment Structures, NUREG/CR-3876

Table 1 Design specification of isolation system

Direction	Property	Value
Horizontal	Initial period T1	1.0 sec
	Isolated period T2	2.0 sec
	Yield coefficient β	0.05
Vertical	Natural period Tv	0.05 sec

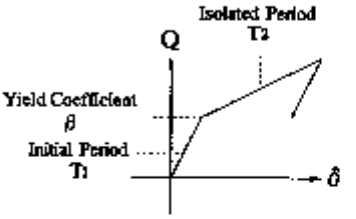

Fig.1 Characteristics of isolation system

Table 2 Considered uncertainties and analysis cases for horizontal response

Uncertainties			Analysis case				
Member	Factor	COV	All Variable	Fc Fix	Khi Fix	Kks Fix	Qhs Fix
Building	Concrete Strength Fc	0.13	Var.*	Fix*	Var.	Var.	Var.
Isolator	Stiffness Khi	0.05	Var.	Var.	Fix	Var.	Var.
Damper	Stiffness Khs	0.03	Var.	Var.	Var.	Var.	Var.
	Strength Qhs	0.10	Var.	Var.	Var.	Var.	Fix
Number of case			100	100	100	100	100

*Var. : Consider its variety Fix : Fix it as mean value

Table 3 Considered uncertainties and analysis cases for vertical response

Uncertainties			Analysis case			
Member	Factor	COV	All Variable	Fc Fix	Kvi Fix	Vs Fix
Building	Concrete Strength Fc	0.13	Var.	Fix	Var.	Var.
Isolator	Stiffness Kvi	0.10	Var.	Var.	Fix	Var.
Soil	Shear Velocity Vs	0.10	Var.	Var.	Var.	Var.
Number of case			100	100	100	100

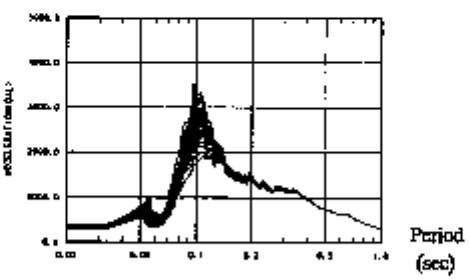

Fig.2 Example of vertical FRS "All Variable"

Fig.3 Evaluation of FRS by Rmax

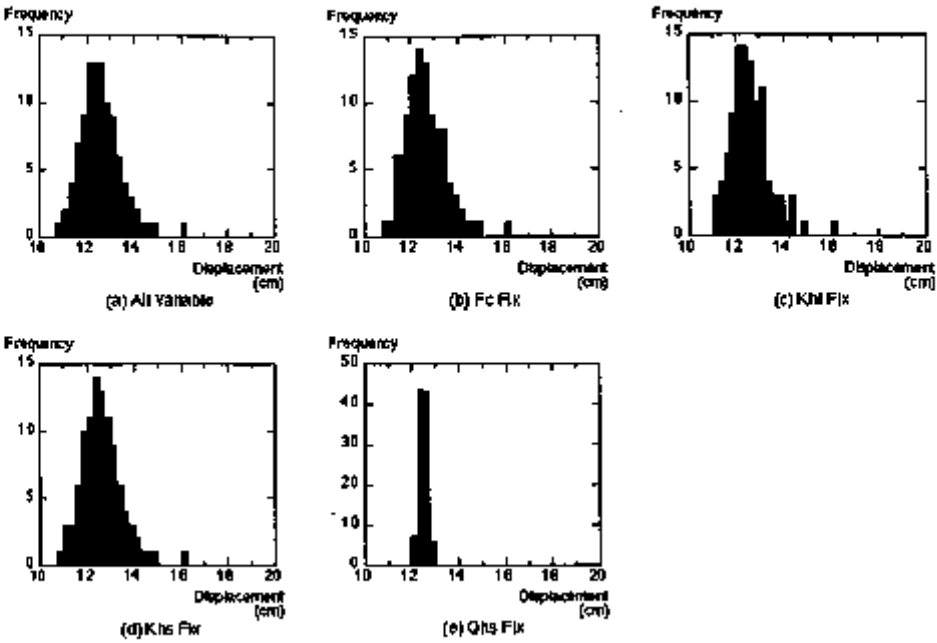

Fig. 4 Distribution of Horizontal Displacement of Isolator

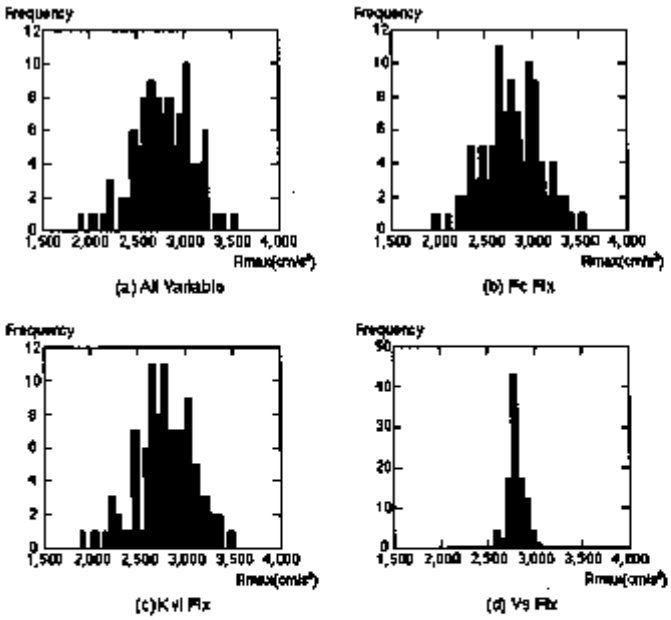

Fig.5 Distribution of Vertical FRS Represented by Rmax

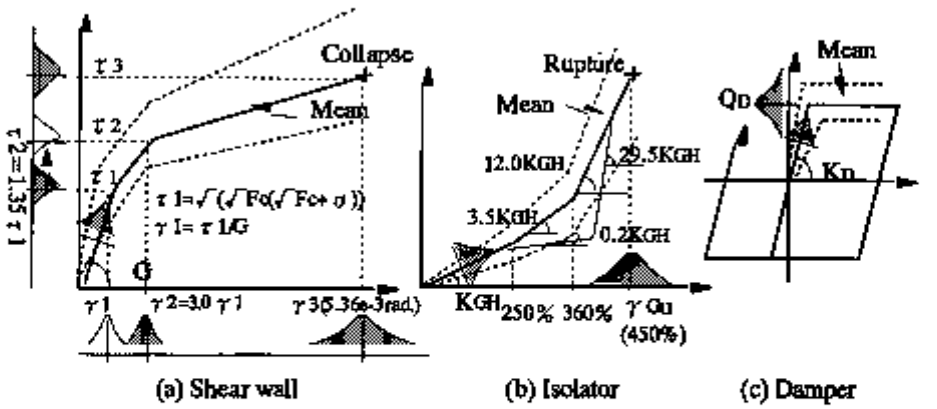

Fig. 6 Variability of skelton curve (structural characteristics).

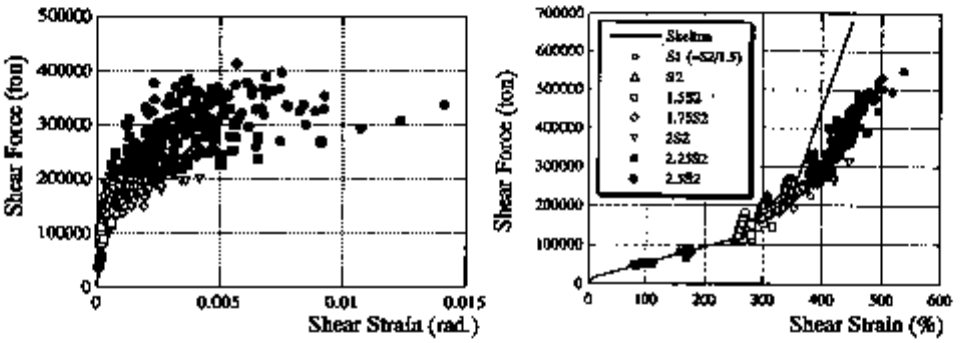

Fig. 7 Results of response analyses at input level S2/1.5 - 2.5S2.

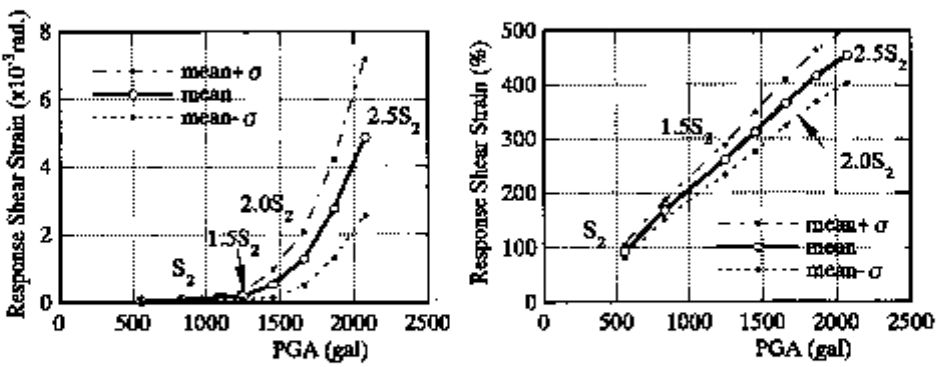

Fig. 8 Mean and standard deviation of response.

Table 4 Results of Fragility assessment

Member	Randomness					Uncertainty	Fragility assessment	
	Response (2.5S2)		Capacity		βR			
	COV	βs	COV	βr	$\sqrt{\beta s^2+\beta r^2}$	βU	Pf*1	HCLPF
8th-story	0.509	0.480	0.31	0.303	0.568	0.15	1.1×10^{-15}	1900gal
7th-story	0.358	0.347	0.31	0.303	0.461	0.15	2.0×10^{-16}	1670gal
6th-story	0.426	0.408	0.31	0.303	0.508	0.15	1.5×10^{-15}	1740gal
5th-story	0.570	0.530	0.31	0.303	0.610	0.15	2.3×10^{-11}	1890gal
4th-story	0.466	0.443	0.31	0.303	0.537	0.15	3.1×10^{-13}	1830gal
3rd-story	0.449	0.429	0.31	0.303	0.525	0.15	9.9×10^{-15}	1730gal
2nd-story	0.452	0.431	0.31	0.303	0.527	0.15	1.7×10^{-13}	1760gal
1st-story	0.472	0.448	0.31	0.303	0.541	0.15	2.5×10^{-11}	1720gal
Iso.-layer	0.113	0.113	0.078	0.078	0.137	0.10	1.4×10^{-8}	1390gal

β : logarithmic standard deviation = $(\ln(1+COV^2))^{1/2}$

*1 :

$$Pf = \Phi\left[\frac{\ln(S/R) + \beta U \Phi^{-1}(0)}{\beta R}\right]$$

in which Pf is the probability of failure, S and R are respectively the mean of response and capacity of a member, and $\Phi(\,)$ is the standard Gussian cumulative function.

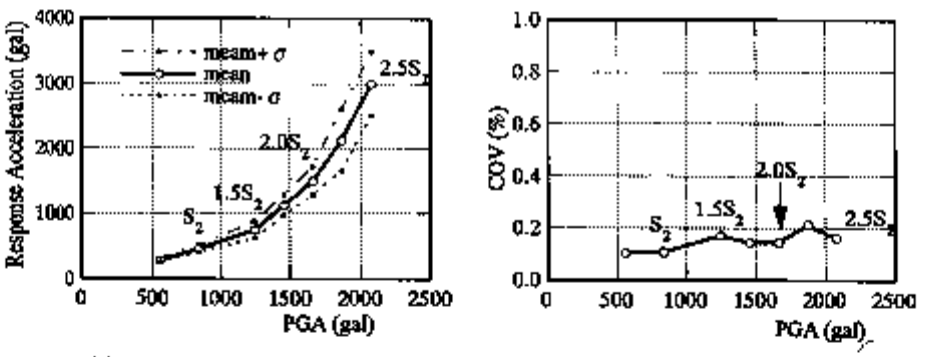

(a) Mean and standard deviation (b) Variability of response acceleration

Fig. 9 Responses at supporting point of Reactor Veseel.

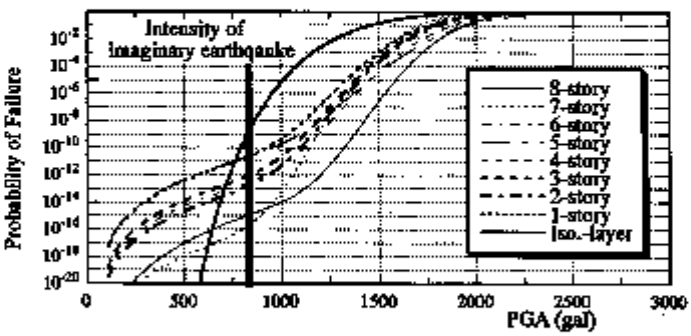

Fig. 10 Fragility assessment for base-isolated reactor building(95% confidence curves).

Transactions of the 14th International Conference on Structural Mechanics in Reactor Technology (SMiRT 14), Lyon, France, August 17-22, 1997 K20/5

Validation of the pseudo-dynamic method to test large scale models of base isolated structures

Renda V., Verzeletti G., Magonette G., Tirelli D., Papa L.
European Commission - Joint Research Centre - ISIS, Italy

ABSTRACT

The research related to seismic risk reduction led, in the last years, to the development of various innovative anti-seismic mechanisms which cover different applications. The efficacy of these devices has been proved by some applications, as shown during the earthquake of Northridge in California, but a systematic use of this technology is made difficult by the absence of design standards. A standard procedure for the Pseudo-Dynamic testing of large scale models of base-isolated structures has been developed and validated at the European Laboratory for Structural Assessment of the Joint Research Centre of the European Commission.

INTRODUCTION

The European Commission (EC) is currently engaged in research activities about the seismic behaviour of structures, the technologies to lower the effects of an earthquake and the verification of the rules for the design standards.

The effects of an earthquake on large size structures are investigated in the European Laboratory for Structural Assessment (ELSA) of the Joint Research Centre (JRC) by means of a Reaction Wall (RW) and the Pseudo-Dynamic (PsD) [1]. The implementation of the PsD method at ELSA is in digital form and allows a very good control of the ramp generation of the target displacements [2]. Presently the main objectives of the laboratory activities are related to the calibration of the rules of the EUROCODE - 8 for the design of steel and reinforced concrete structures [3].

The EC is interested in the follow-up of innovative techniques and mechanisms for seismic risk reduction to verify the effectiveness of the technology, the reliability of the mechanisms and to contribute to the development and validation of the related design rules and standards.

To this end a collaboration has been set up with the Italian Working Group on Seismic Isolation which contributed to the present work.

BASE ISOLATION IN EARTHQUAKE ENGINEERING

In the last years an important effort was done to improve the design capabilities for earthquake engineering and it led to the set up of design standards for seismic areas. Another line of research has been followed with the aim of investigating innovative ways for the control of the induced vibrations. The investigation led to the development of innovative passive anti seismic devices. These are essentially related to the technology of base isolation and energy dissipation.

These two different types of devices can be considered complementary to each other. Base isolation is finalised to the reduction of the frequencies of the structure in order to escape the range of frequencies inducing high acceleration due to resonance, while energy dissipation devices are finalised the protection of the carrying structures by lowering the energy transmitted to them.

The efficacy of base isolation is relevant for hard soils or in general with a frequency capacity of transmissibility spectrum with high acceleration in the range of some Hertz, while it is low for sandys soils or with a spectrum with high acceleration in the range below one Hertz. where for those cases, energy dissipation is more effective. The base isolation technology is well developed, but the its application in earthquake engineering is made difficult by the absence of design rules for isolated structures. To overcome this gap there is the necessity of tests on large scale models of structures to develop and validate the design standards.

VALIDATION OF THE PsD TEST METHOD

In principle there is no doubt about the applicability and the potentiality of the PsD method; the problem is the influence of the test velocity on the characteristics of the isolator material; some literature exists on the subject and probably the influence of strain rate is not such to invalidate the results of a PsD test; moreover, this problem is probably dependent on the isolator materials.

At this stage some structures existing at ELSA have been reused to improve and validate a standard procedure for the PsD testing of base-isolated structures. Because the structures existing at ELSA will be tested in the framework of the planned activity of the laboratory, these structures must thus be repaired before being tested in the framework of the Seismic Isolation Programme. Some additional investigations (as the comparison with the original eigen-frequencies, stiffness matrix, etc.) will be performed to verify the integrity of the structure before the reuse to test using base-isolation devices.

The main aim is to set-up a self-standing validated procedure. In a second stage also a comparison between a dynamic shaking table test and a PsD test will be performed. This will be done only for a small-scale model of structure tested at the laboratory of ISMES, owner of a shaking table, and at ELSA.

EFFECT OF THE STRAIN RATE

The PsD method is based on a quasi-static load application by means of hydraulic actuators acting on selected point of the structure which is connected to the strong floor of the laboratory. The seismic effect is correctly simulated being the differential displacements evaluated by a computer solving,

step by step, the equations of motion. Potentially the method is very attractive for structures with masses lumped at the point of application of the actuators and for materials whose behaviour is independent of the strain rate. This last point is not the case for the materials used for the base isolators. To overcome this difficulty is very important for the reliability of the test results; at ELSA a standard procedure to validate the rate-sensitivity of materials has been set up [4].

As it is known, that the PsD method is an hybrid numerical-experimental approach for the solution of the complex structural analyses problems. The basic idea is that the reaction forces measured during the test at the top of the isolators could be multiplied for a correction factor to be introduced in the numerical part of the method [5]. In principle this numerical correction factor is dependent on the materials and on the difference between the strain rates during the real dynamic load application and the PsD quasi-static application.

It has been shown at ELSA that this correction factor can be evaluated by a characterization of the isolators for application of loads with different strain rates. Only few characterization tests can be enough to reach the goal providing that the loads are applied with the same ratio in time scale between the PsD test and the dynamic one (usually this ratio at the ELSA tests is of two orders of magnitude).

STANDARD TEST PROCEDURE

To overcome the difficulties due to the strain rate dependency for testing base-isolated structures, the following standard procedure has been set-up at ELSA:

- characterization of the isolators and assessment of the correction factor for PsD tests;
- dynamic snap-back;
- PsD snap-back assuming the correction factor assessed by the characterization tests;
- comparison of the results obtained from the dynamic and PsD snap-back tests and validation of the procedure;
- tests for earthquake signals with the PsD numerical method implemented to account for the correction factor.

This standard procedure is self consistent and allows the validation case by case. In fact the dynamic snap-back is a reference case for the corrected PsD test of the structure and the isolators under examination.

CHARACTERIZATION TESTS OF THE ISOLATORS

General considerations

The activity is finalized not only to the intrinsic characterization of the isolators, which is of relevant importance, but also to the quantification of the effect on strain rate dependency of the horizontal shear of the isolators.

Usually, for common building materials, the errors introduced by a PsD test may be disregarded since they are less important than the existing variability from specimen to specimen. However, for

the isolators, a decrease of testing speed of two or three orders of magnitude –as is usual for a PsD test-- may introduce considerable changes in the stress-strain behaviour, especially for filled rubber.

To compensate for this effect, at every step of the PsD integration, the measured forces may be corrected so as to account for an increase of a specified percentage of the isolators stress. To this end a correction coefficient to be implemented in the PsD numerical algorithm for the tests to be performed, is obtained experimentally before hand. The experimental arrangement for the characterisation tests is shown in Fig. 1.

Four isolators are placed in a two-by-two symmetric position and bolted to a mobile apparatus which applies controlled displacements. The tests allow the plotting of the shear force as a function of the displacement at the top of the isolators. The imposed histories are sinusoids of various frequencies.

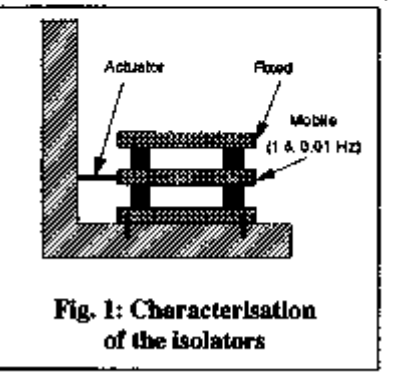

Fig. 1: Characterisation of the isolators

In practical applications, the aim of isolation is to shift the first frequency of the over-standing structure in the low frequency range (in general less than 1 Hz) to escape the range of the higher values of acceleration in the earthquake response spectrum. The PsD tests are in general, done with a time scale of about one two-to-three hundreds orders of magnitude slower than the real dynamic case. For the above mentioned reasons the characterization tests are done in the low frequency range and assuming a ratio of the boundary frequencies equal to the ratio in time scale between the dynamic and PsD tests.

Isolator geometry and materials

The isolator devices were rubber bearings with a diameter of 250 mm and made of 11 rubber layers with a thickness of 6 mm (66 mm of total rubber height), 10 steel layers of 1.5 mm (alternating between the rubber layers) and two end steel plates of 10 mm which included threaded holes for fixation. Consequently, the total height of each isolator was of 101 mm. The isolator is shown in Fig. 2. The isolators were designed for a working shear strain of 100% (66 mm of horizontal displacement) and a nominal vertical load of 400 kN. Four of these isolators, made of a high-damping rubber mixture called EN60, were made available to ELSA for this test campaign. The results of the characterization tests are shown in Fig. 3.

From these results a bearing shear force of the order of 20% was adopted as correction factor. The figure shows the results for times of 10s and 1000 second; for the last case, the results with the correction factor of 20% is compared with the curve for 1 s. The two curves are very close each other.

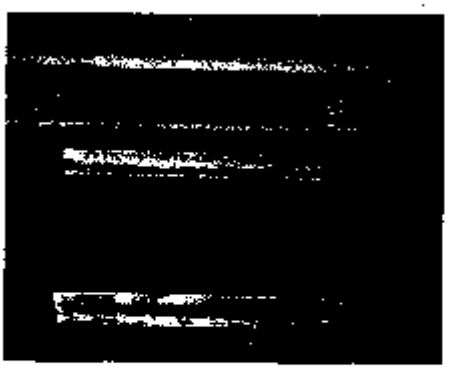

Fig. 2: Isolator

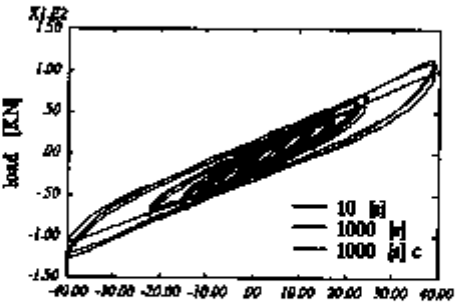

Fig. 3: Characterisation results

DYNAMIC AND PsD SNAP-BACK

The execution of a dynamic snap-back is the second step of the standard procedure. The aim is to obtain a reference data for a PsD simulation accounting for the correction factor in order to validate the PsD tests.

Description of the structure mounted on the isolators.

The structure is a three storey steel frame with a total height of 10.40 m, 5.00 m wide and 5.00 m deep [6] which had been previously used for several test campaigns without isolation and repaired afterwards. The steel frame is shown in Fig. 4.

Fig. 4: Steel frame

Each floor of the structure is made of a concrete slab to which two hydraulic actuators were attached (only the front one is seen in the figure). Since the bases of the columns were no longer resting on a rigid foundation, each frame was closed by a stiff beam with the same profile (HEB 400) as the columns and these beams constituted the base floor which was fixed onto the four isolators positioned at the corners. This new base - which will be called here floor 0 - was also provided with an additional concrete block of about 250 kN of weight to which a single actuator was attached. The main function of this block was to increase the total weight of the specimen, which was of about 750 kN. Although this load was only about one half of the design vertical load of the isolator set, it was considered sufficient for the purpose of these tests since the addition of more heavy blocks would have considerably increased the cost of the set up.

The snap-back has been simulated by means of the PsD method in the two cases with and without correction factor applied at the shear forces at the top of the isolators. The correction factor of 20% is included in the numerical algorithm of the method. The results are shown in Fig. 5.

Also the comparison with the Dynamic test is included. The results have shown that the PsD test without correction have significant differences compared with the dynamic one. This is in agreement with the results of the characterization tests. In particular the most relevant difference is in frequency.

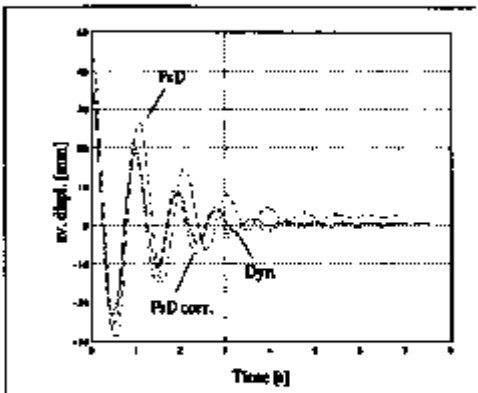

Fig. 5: Dynamic and Psd snap-bak

The results obtained assuming the correction factor of 20% in share force of the isolator are very near to those related to the dynamic tests. The frequencies are close to each other as shown also b the behaviour of the 1st mode frequency spectra. It was found that the acceleration peak is at frequency of about 1.2 Hz for the dynamic and corrected PsD tests, while it is of about 1 Hz for th PsD without correction.

PSEUDO-DYNAMIC SEISMIC TESTS

The above described experimental tests have shown the possibility to correct in a suitable way th response of the isolators to account for sensitivity of the material to the strain rate effect. Finally th PsD settings obtained from the previous tests have been used to perform PsD tests on the steel fram for a seismic input. The aim of the work is to have a first assessment of the effectiveness of th isolation for a large scale base isolated model that is representative of a realistic situation. The goal reached by comparing the results obtained with and without the isolation applied at the bottom of th structure. As input it has been assumed the accelerogramme of Kalamata, shown in Fig. 6, amplifie for a factor 1.5.

It has been used an elastic spectrum with 5% of damping. The zone of resonance is in the range of 3.2 Hz. Previous experiments on the frame, without isolation, showed a first frequency of 3.96 Hz, whereas the isolated structure has a first frequency of about 1.2 Hz. This first comparison gives a first qualitative indication of the effectiveness of the isolation for the case under examination.

The comparison between the results obtained at the three floors for the two configurations with and without isolation is shown in Fig. 7, Fig. 8 and Fig. 9.

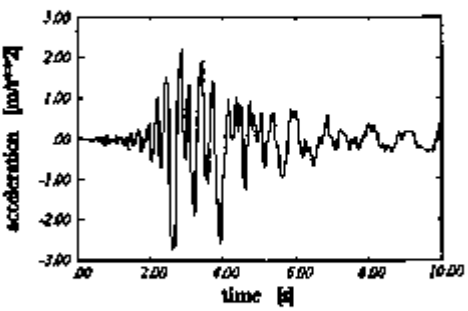

Fig. 6: Kalamata signal

The comparison highlights the strong reduction of the forces, proportional to the accelerations, due to the isolation. The maximum load at the third floor of the order of 700 kN without isolation is drastically reduced to about 100 kN for the isolated structure.

Also the diagrams of the shear loads versus the inter-storey drift showed a relevant decrease both in drift and shear due to the isolation. In particular, for the third floor the inter-storey drift is lowered from about 55 mm without isolation to about 15 mm with isolation. A certain amount of energy is dissipated by a non-linear hysteretic behaviour of the material of the frame in the configuration without isolation, while the behaviour remains elastic in the case with isolation.

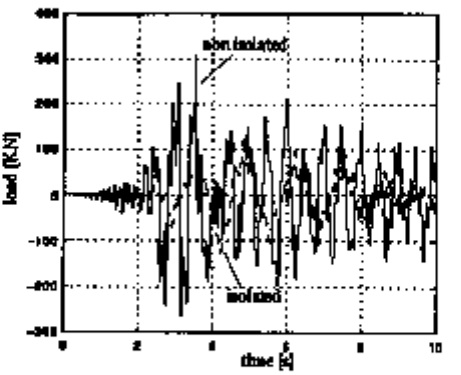

Fig. 7: comparison at the first floor

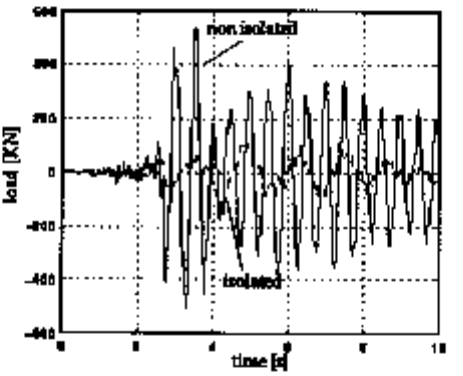

Fig. 8: comparison at the second floor

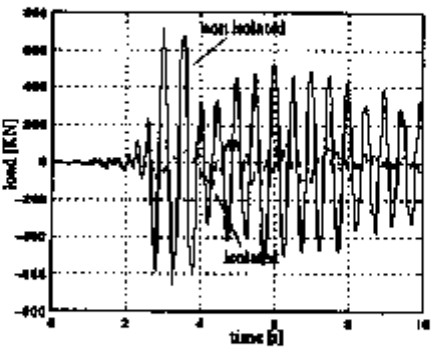

Fig. 9: Comparison at the third floor

CONCLUSION

The work performed at the Joint Research Centre of the European Commission, in collaboration with the Italian Working Group on Seismic Isolation, was finalised to show the possibility of PsD testing of isolated structures and to make available a standard procedure to this end.

The main problem is the strain rate sensitivity of the isolator materials which could affect the reliability of the results. The experimental activity showed the possibility to set-up a standard procedure to obtain an intrinsic validation, case by case, of the tests. This is possible because of the flexibility of the PsD methodology which is a mixed numerical-experimental one. The numerical part allows the possibility to correct, step by step, the measured restoring forces before their usage in the numerical algorithm. To reach this objective, a characterisation test of the isolators for various frequencies allows the definition of a correction factor to be applied to the measured restoring forces at

the top of the isolators. This correction factor depends essentially by the strain rate ratio between the dynamic behaviour and the PsD simulation. The comparison of a dynamic snap back test with a PsD simulation allows a very good setting-up of the corrected PsD model. The results obtained for the Kalamata earthquake, and verified also for others seismic inputs, showed a relevant efficacy of the isolation technology applied to realistic structures.

In conclusion a tool has been make available, based on a big Reaction Wall and the PsD method to test base isolated, large scale, structures and to contribute to the verification of the design of relevant projects and the development and validation of standard rules for the design of base isolated structures.

LIST OF REFERENCES

[1] Donea, J., Jones, P.M., Magonette, G., and Verzeletti, G., "The pseudo-dynamic test method for eathquake engineering: An overview", European Commission, EUR 12846 EN, Brussels.

[2] Magonette, G., 1991, "Digital control of pseudo-dynamic tests", Experimental and numerical methods in earthquake engineering, Kluwer academuc press, pp. 63-69.

[3] Negro, P., Verzeletti, G., Magonette, G., and Renda, V., 1994, "Pseudodynamic testing of a four-storey full-scale reiforced concrete frame building design in accordance with Eurocodes 2 and 8.", 10-th European Conference on Earthquake Engineering, AUG. 28 - SPT. 2, Vienna Austria.

[4] Gutierrez, E., Magonette, G., and Verzeletti, G., 1993a, "Experimental studies of loading rate effects on reinforced concrete columns", ASCE Journal of engineering mechanics, 119, pp 887-904.

[5] Gutierrez, E., and Verzeletti, G., 1993, "Possibilities of vibration isolation testing at the ELSA laboratory of the Joint Research Centre", Proceedings of the XII Post SMiRT Conference on Isolation, Energy Dissipation and Control of Vibrations os Structures, Capri, Italy.

[6] Kakaliagos, A., 1994, "Pseudo-dynamic testing of a full scale three-storey one-bay steelmoment-resisting frame. Experimental and analytical results", EC, JRC, IST Report EUR 15605 EN., Brussels.

[7] Renda, V., Martelli, A., Verzeletti, G., and Papa, L., 1995a, "Research activities and programmes on Seismic Isolation at the Joint Research Centre of the European Commission" 13-th Post SMiRT specialized conference, 21-23 AUG., Chile.

[8] Renda, V., Verzeletti, G., and Papa, L., 1995, "A European collaboration Research Programm to study and test Large Scale Base Isolated Structures", 13-th SMiRT, 13-18 AUG., Port Alegre, Brasil.

Transactions of the 14th International Conference on Structural Mechanics in Reactor Technology (SMiRT 14), Lyon, France, August 17-22, 1997 K11/2

A study of vertical seismic responses for base isolated PWR using high damping rubber bearing

Yoo B.[1], Lee J.H.[2], Koo G.H.[1], Kim Y.H.[2]
(1) Korea Atomic Energy Research Institute, Korea
(2) Korea Advanced Institute of Science and Technology, Korea

ABSTRACT

Time history analyses of a base isolated Pressurized Water Reactor(PWR) building with high damping rubber bearings as isolator are performed to evaluate seismic responses for two earthquakes. While the horizontal acceleration responses in base isolated superstructure are much smaller than those in fixed base structure, the vertical accelerations of the superstructure are amplified to some extent. Sensitivity study to reduce vertical responses at superstructure is carried out by manipulating the vertical stiffness and damping of isolation system.

1. INTRODUCTION

The seismic isolation systems used for the reduction of the seismic response of the structures are now practically applied in Japan, USA, New Zealand, Italy, China, etc. where large earthquakes are occurred. In Korea a seismic isolation system was applied for LNG tanks, and authors have studied to establish the seismic isolation design for nuclear facilities[1,2]. Horizontal seismic base isolation system is excellent to reduce the horizontal seismic responses but likely tends to amplify the vertical responses[3]. To resolve the problem some ideas for vertical isolation systems[4,5,6] have been suggested such as helical springs and viscodampers, air springs and horizontal rubber bearings, multicomponent low frequency system. Since high damping laminated rubber bearing(HLRB) has a comparably large damping, the accelerations in superstructure are remarkably reduced in horizontal direction[1,2,3]. However the vertical stiffness of HLRB to transmit vertical load is relatively larger than horizontal one, the seismic responses in vertical direction are likely to be amplified. Thus vertical behavior of HLRB on seismic responses of superstructure should be evaluated.

In this paper, simplified linear two DOF isolation system are studied and time history analyses for a typical PWR superstructure with a HLRB isolation system are performed to understand the effects on the seismic responses in superstructures and the results are compared to fixed base model. Sensitivity study to reduce the vertical responses at the superstructure is carried out by manipulating the vertical stiffness and damping of isolation system. Vertical isolation system with soft stiffness and high damping may meet the tentatively proposed vertical isolation criteria that requires the vertical acceleration response at the critical support of the superstructure be not larger than zero period acceleration(ZPA) of input motion.

2. STRUCTURAL MODEL

The model for isolated PWR containment structure used in the analysis is shown in Fig.1. The isolated system considered in this paper consists of the isolator, base mat and the superstructure (containment vessel part and internal structure part). The computer program used in analysis is ABAQUS version 5.5[7].

In the model, the nodes from 1 to 10 represent the containment part and the nodes from 11 to 17 represent internal structure part. The nodes 18, 7 and 11 represent the base mat, the polar crane support and the reactor vessel support respectively. The total weight of the superstructure is about 68,000 tons. The structural damping of the superstructure is assumed to be material damping with 5% damping ratio for all modes.

Fig.2 shows the shear cycle test results of the HLRB, which is scaled down 1/8 size. In modeling of the isolator which has severe hardening characteristics in large strain region, a non-linear spring model with an equivalent viscous damping should be applied. However, the shear deformation predicted in the analysis is much smaller than 150% shear strain up to which is assumed to be linear, we can use an equivalent linear spring model for horizontal direction as follow:

$$Kh = 0.6887 \times 10E6 \text{ Kgf/cm.}$$

The Kh is determined by an equivalent stiffness that is resonated at 0.5Hz in horizontal direction. The vertical stiffness of isolator is designed to resonate at 21 Hz as follow:

$$Kv = 1214.9 \times 10E6 \text{ Kgf/cm.}$$

The vertical stiffness is assumed to be in compression state because it always resists total structure weight. The viscous damping values of the isolator used for the numerical simulations are 12% for horizontal direction, and 12%, 5%, and 0% for vertical one.

3. DYNAMIC CHARACTERISTICS OF SUPERSTRUCTURE

In horizontal direction, the fundamental frequencies of the containment building and internal structures for fixed base are 5.39 Hz and 15.73 Hz respectively, and for base isolated system are 5.94 Hz and 16.17 Hz respectively. The horizontal isolated frequency of the isolation system is 0.5 Hz. Fig.3 shows the first seven modes of the base isolated model in horizontal and vertical directions.

In vertical direction, the fundamental frequencies of the containment vessel and internal structures for fixed base are 12.15 Hz and 26.8 Hz respectively, and for base isolated system are 11.42 Hz and 27.95 Hz respectively, and the vertical natural frequency of the isolation system is 21Hz. Table 1 and Table 2 show the several frequencies of the models.

4. EFFECTS OF ISOLATOR ON STRUCTURAL RESPONSES UNDER EARTHQUAKES

4.1 Linear Two DOF Isolation System Study

To investigate the role of isolation frequency and damping on the seismic responses, we introduced 2 degrees of freedom system simulating the PWR superstructure that is isolated and applied white noise input, and two structural frequencies, 5Hz and 15Hz are considered. Several mass ratios that are effective masses of each mode divided by the effective isolation mass are taken into account in this analysis. As increasing of isolation frequency as shown in Fig. 4, the acceleration response ratios between isolated and fixed base structure of this 2 DOF structure with 12% isolation viscous damping are increased monotonously, but the relative

displacement response ratio is decreased asymptotically. The acceleration response ratios of 2 DOF structure isolated with 0.5Hz are reduced as increase of the isolation damping values as shown in Fig. 5.

4.2 Effects of Isolators on PWR Seismic Responses

The isolated system is assumed to be subjected to horizontal and vertical component of 1940 El Centro earthquake and artificial one compatible to USNRC RG1.60 design response spectra as shown in Fig. 6. The effects of the isolator on the superstructure responses are investigated by using the numerical simulations.

In Table 3 the horizontal ZPAs at the superstructure for the isolated system, which represents rigid body motion, are remarkably reduced to 0.125g at reactor support and 0.13g at polar crane support when it is subjected to peak ground acceleration(PGA) of 0.34g horizontal El Centro earthquake(NS). It is noteworthy that the acceleration at the crane support for the fixed base system is 0.97g and that at reactor support is 0.34g respectively. In case of SSE 0.3g artificial one the horizontal ZPAs at the superstructure for the isolated system are also reduced to 0.172g at reactor support and 0.179g at polar crane support from 0.38g and 1.24g in fixed base model.

The vertical seismic responses of superstructure with horizontal isolator subjected to PGA of 0.2g vertical El Centro earthquake and SSE of 0.21g vertical artificial one are represented in Table 4. The vertical ZPAs at the superstructure for the isolated system without vertical isolator are increased to 1.0g and 0.7g at polar crane support while those for the fixed base system are 0.81g and 0.61g respectively. Since high vertical stiffness of horizontal isolator has vertical natural frequency as 21 Hz which cannot make the participation factor of the first superstructure mode lower. Hence the vertical response of the structure cannot be reduced but amplified with this high vertical stiffness of isolator because the first vertical superstructure mode corresponds to the high spectral value of the vertical input motions.

In order to reduce the vertical response of the superstructure, the several analyses are performed by changing the vertical stiffnesses for the natural frequency of the vertical isolation system to be in the frequency range of 5 Hz to 1 Hz. The results are summarized in Table 5 & 6, and Fig. 7 & 8. Under these softer stiffnesses the vertical ZPA varies depending on the seismic input types, isolator damping values and superstructure dynamic characteristic features. The higher damping is effective to reduce the acceleration and displacement responses, but the vertical damping device is not easily available. So the soft stiffness is another choice to reduce the acceleration, but it is important to consider the seismic input spectrum and the first frequency of superstructure because the vertical isolation frequency around of 5Hz under the artificial seismic input amplifies their vertical responses as shown in Fig. 8. On the contrary softening of vertical isolation frequency, lower than fundamental frequency of structure, always reduces the acceleration responses as verified in two DOF isolation system study.

We suggest the isolation criteria that the acceleration response at the critical support of superstructure be at least not larger than ZPA of input motion. Horizontal isolation system with high damping rubber bearing currently developed is effective in reducing horizontal seismic responses but amplifies vertical seismic responses. Based upon the results of sensitivity study as shown in the Table 5 & 6, as the vertical isolation frequency is lowered to 5 Hz from 21 Hz which is the vertical natural frequency of horizontal isolation system, the acceleration responses at the superstructure are decreased, but are not so sufficiently reduced to satisfy the requirements. If we reduce the isolation frequency less than 1 Hz or 2 Hz and

increase the damping of vertical isolation system more than 5%, we may obtain the vertical seismic responses which meet the criteria.

Meanwhile the vertical displacement is increased as we lower the frequency of vertical isolation system and is decreased as we enlarge the damping of vertical isolation system.
Now we are developing 3 dimensional isolation system which can reduce the horizontal acceleration responses as well as the vertical ones under the following considerations for implementation of proper 3D isolation; 1) integral isolator with function of both horizontal and vertical isolation, 2) need to decouple the vertical and horizontal isolation roles, 3) need to be passive system.

5. CONCLUSIONS

The acceleration responses in base isolated PWR superstructure with HLRB isolator subjected to 1940 El Centro earthquakes and artificial ones compatible to USNRC RG 1.60 spectra are much smaller than those in fixed base superstructure in horizontal direction. But the vertical acceleration responses are larger than those in fixed base superstructure. Tentative vertical isolation criteria which requires that acceleration responses at the critical support of superstructure in this case at the reactor support be not larger than ZPA of input motion is proposed. Vertical seismic isolation with the reduced vertical stiffness and large damping of isolator is more effective in reducing the vertical seismic responses. In the base isolated system, the seismic acceleration responses at flexible structure are much more reduced than those at stiff structure.

The further researches to implement the vertical isolation design for the reduction of vertical seismic responses, and to study the rocking behavior induced by vertical flexibility are needed.

REFERENCES

1. Yoo, B., Lee,J.H., Koo,G.H. and Kim,Y.-H. 1995. Effects of High Damping Rubber Bearing on Seismic Response of Superstructure in Base Isolated System.
13-th SMiRT, Brazil.
2. Yoo, B., Lee,J.H., Koo,G.H. and Lee,D.G. 1995. Seismic Isolation for Nuclear Reactors in Korea.
Int. Post-SMiRT Conf. Seminar on Seismic Isolation, Passive Energy Dissipation and Control of Vibrations of Structures, Santiago, Chile.
3. Tajirian, F.F. and Patel, M.R. 1993. Response of Seismic Isolated Facilities: A Parametric Study of the ALMR.
12-th SMiRT, Stuttgart, Germany.
4. Hueffmann, G.K. 1991. Base Isolation of Two Residential Buildings in Los Angeles with Helical Springs and Viscodampers.
11-th SMiRT Post Conference Seminar on Seismic Isolation, Japan.
5. Tokuda, N., et al, 1995. Three Dimensional Base Isolation System for Assumed FBR Reactor Building.
13-th SMiRT, Brazil.
6. Beliayev, V.S, Vinogradov, V.V. 1995. Optimization of Power Characteristics of Multicomponent Low Frequency System of Seismic Protedction of Building with Reactor Plant of VVER-600 Type. 13-th SMiRT, Brazil.
7. ABAQUS Version 5.5, Standard User's Manual I,II.

Table 1. Horizontal Natural Frequencies of PWR Reference Plant

	Fixed base			Horizontal isolator with 0.5 Hz		
Mode No	Frequency (Hz)	Parti. factor	Effect. Mass (kg)	Frequency (Hz)	Parti. factor	Effect. Mass (kg)
1	5.386	1.470	15.11E06	0.5*	1.0106	68.34E6
2	15.73	1.532	14.43E06	5.94	-0.0112	942.0
3	16.24	-0.452	1.926E06	16.17	-0.0001	0.257
4	22.38	0.246	3.370E06	17.77	-0.0012	16.36
5	30.68	-0.391	0.657E06	23.76	-0.0003	3.568

* : Horizontal Isolation Frequency of Horizontal Isolator

Table 2. Vertical Natural Frequencies of PWR Reference Plant

	Fixed base			Vertical(21Hz)*			Vert. Isolator with 5.0Hz		
Mode No.	Freq. (Hz)	Parti. Factor	Effect. mass	Freq. (Hz)	Parti. factor	Effect. mass	Freq. (Hz)	Parti. factor	Effect. mass
1	12.15	1.511	20.91E6	11.42	1.778	33.23E6	4.85**	1.180	67.85E6
2	26.80	-0.719	4.246E6	22.0*	-1.227	29.39E6	14.68	-0.201	0.392E6
3	32.20	1.323	15.53E6	27.95	0.382	1.766E6	27.52	0.002	2990.0

* : Vertical Frequency of Horizontal Isolator

** : Vertical Isolation Frequency of Vertical Isolator

Table 3. Horizontal Responses under El Centro(0.34g) and Artificial Time History(0.3g)

Input Motion	El Centro(NS)			Artificial time history of USNRC		
Isolator frequency	Fixed	0.5 Hz		Fixed	0.5 Hz	
Viscous damping	-	12%	0%	-	12%	0%
RV support(g)	0.340	0.125	0.172	0.383	0.172	0.272
Polar crane(g)	0.970	0.130	0.182	1.244	0.179	0.273
Isolator displ.(cm)	-	12.8	17.9	-	19.8	30.8

Table 4. Vertical Responses under El Centro(0.2g) and Artificial Time History(0.21g)

Input Motion	El Centro(Vertical)					Artificial time history(Vertical)				
Isolator frequency	Fixed	21 Hz				Fixed	21 Hz			
Viscous damping		25%	12%	5%	0%		25%	12%	5%	0%
RV support(g)	0.328	0.387	0.462	0.511	0.551	0.216	0.260	0.287	0.304	0.319
Polar crane(g)	0.806	0.841	0.904	0.954	1.00	0.605	0.620	0.651	0.662	0.700
Isolator displ.(cm)	-	0.025	0.027	0.028	0.030	-	0.018	0.021	0.021	0.021

Table 5. Vertical Responses of EL Centro Vertical Seismic Input(0.2g)

		Vertical isolation frequency								
Isolation frequency	Fixed base	5 Hz			2Hz			1Hz		
Viscous damping		12%	5%	0%	12%	5%	0%	12%	5%	0%
RV support(g)	0.328	0.216	0.292	0.444	0.132	0.151	0.228	0.036	0.050	0.084
Polar crane(g)	0.806	0.274	0.367	0.532	0.134	0.150	0.233	0.040	0.051	0.084
Upper base(g)	0.210	0.209	0.287	0.438	0.132	0.151	0.227	0.036	0.050	0.084
Isolator displ.(cm)	-	0.220	0.309	0.466	0.786	0.930	1.42	0.878	1.232	2.11

Table 6. Vertical Seismic Responses of an Artificial Time History USNRC Vertical Input(0.21g)

		Vertical isolation frequency								
Isolation frequency	Fixed base	5 Hz			2Hz			1Hz		
Viscous damping		12%	5%	0%	12%	5%	0%	12%	5%	0%
RV support(g)	0.216	0.383	0.543	1.322	0.270	0.399	0.625	0.150	0.191	0.303
Polar crane(g)	0.605	0.446	0.619	1.497	0.280	0.414	0.641	0.150	0.193	0.305
Upper base(g)	0.208	0.379	0.536	1.303	0.269	0.398	0.624	0.150	0.191	0.303
Isolator displ.(cm)	-	0.393	0.561	1.369	1.636	2.488	3.905	3.487	4.79	7.518

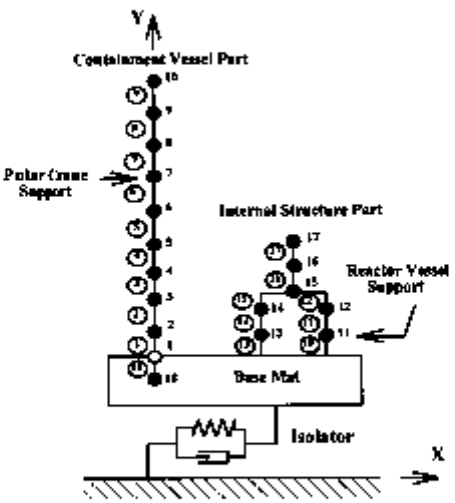

Fig. 1 Model of PWR Reference Plant

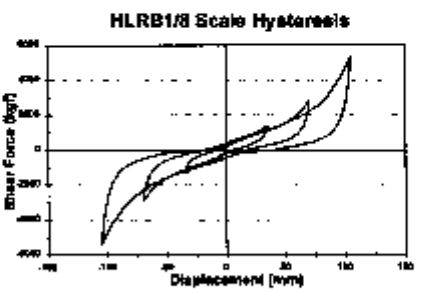

Fig. 2 Hysteretic Curve of 1/8 Scale HLRB

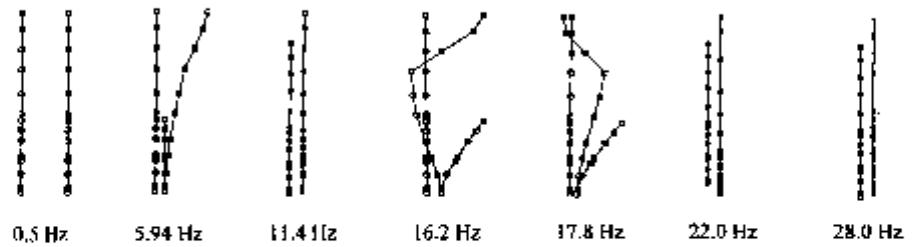

Fig. 3 Mode Shapes of Superstructure Base-Isolated with 0.5 Hz

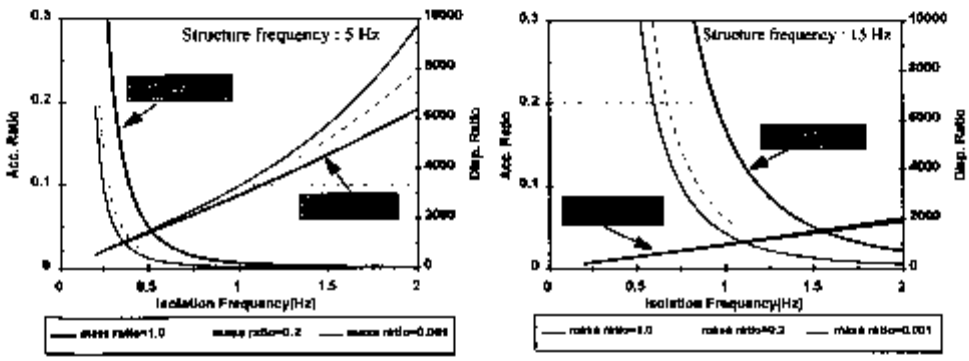

Fig. 4 2 DOF Superstructure Responses with Isolation Frequency
(Isolator Viscous Damping: 12%)

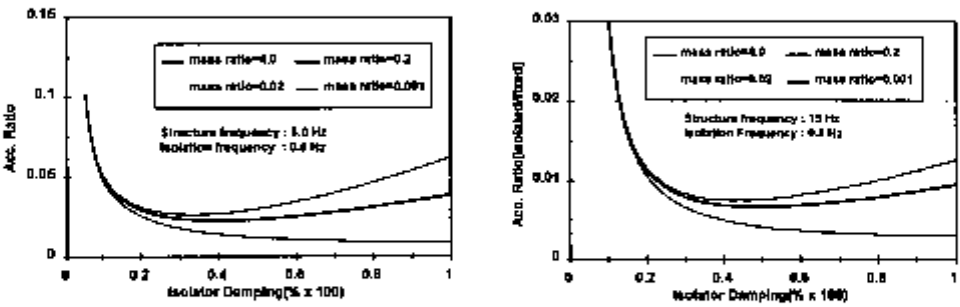

Fig. 5 2 DOF Superstructure Responses with Isolator Damping

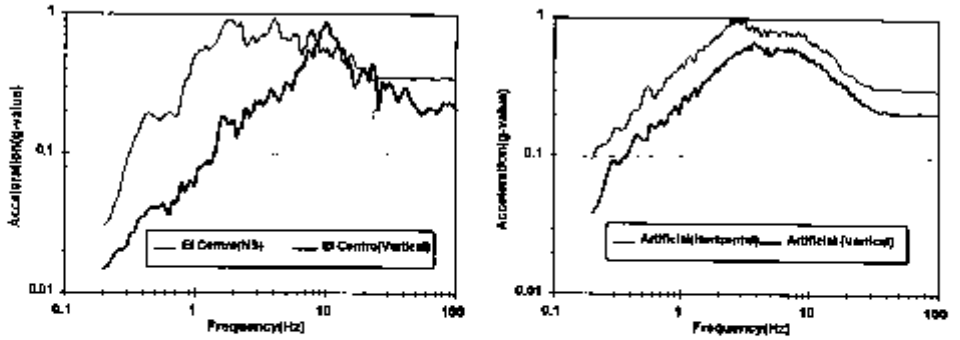

Fig. 6 Acceleration Input Spectra of 1940 El Centro and Artificial Earthquakes

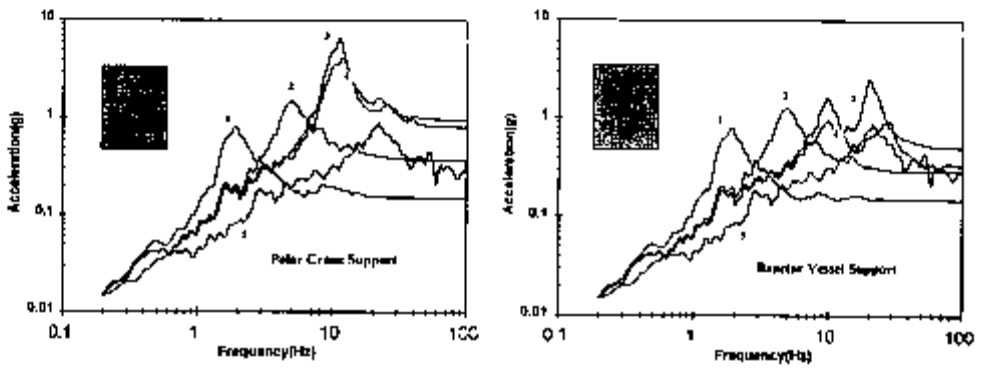

Fig. 7 Vertical Acceleration Response of Superstructure under El Centro Earthquake

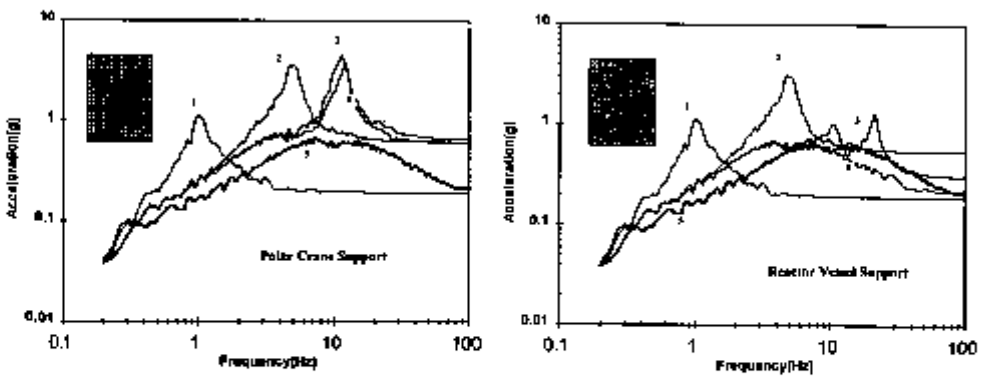

Fig. 8 Vertical Acceleration Response of Superstructure under Artificial Earthquake

Transactions of the 14th International Conference on Structural Mechanics in Reactor Technology (SMiRT 14), Lyon, France, August 17-22, 1997 K12/4

Experimental and numerical evaluation of benefits of optimized HDRBs for seismic isolation

Dusi A(1), Bettinali F.(1), Forni M.(2), Martelli A.(2), Indirli M.(2), Bonacina G.(3), Pucci G.(3), Marioni A.(4), Mazzieri C.(5)
(1) ENEL S.p.A. - CRIS, Italy
(2) ENEA, Italy
(3) ISMES S.p.A., Italy
(4) ALGA S.p.A., Italy
(5) Ansaldo - Ricerche S.R.L., Italy

ABSTRACT: Presented in this paper are the main features and results of the experimental and numerical studies which were performed by the Italian partners in a research project funded by the European Commission, to evaluate the benefits related to the use of optimized High Damping Rubber Bearings as seismic base isolators on the design of structures.

INTRODUCTION

It has been mentioned in a separate paper [1] that, in the framework of the studies performed in Italy on seismic isolation (SI), a 30 months research project [2], funded by the European Commission (EC) and aimed at developing optimized High Damping Rubber Bearings (HDRBs) and evaluating the benefits of their use on the design of structures of various kinds (including nuclear plants), was completed in 1996. It has also been mentioned in [1] that the contributions of the Italian partners to this project comprised (among others) wide-ranging tests and detailed numerical analyses of (a) rubber specimens and single isolators, and (b) isolated structures [2-8].

This paper summarizes the activities concerning item (b) and reports some of the most recent results, while the separate paper [1] deals with the R&D work related to item (a). More details, with respect to those given in this paper, will be provided in ref. [9].

ANALYSED STRUCTURES

The Italian partners in project [2] (ENEL, ENEA and ALGA) contributed to the evaluation of benefits of SI systems formed by optimized HDRBs by performing experiments on two structure mock-ups at ISMES and ANSALDO-Ricerche (ARI) and by numerically analysing the results of both such experiments and those of on-site tests which had been previously carried out by them on actual buildings [3, 7, 8].

Mock-up experiments consisted of shake table tests of ENEL at ISMES on the MISS (Model of Isolated Steel Structure) mock-up, which has a flexible superstructure (Fig. 1a), and pull-back tests of ALGA at ARI on a mock-up having the same rigid superstructure as in previous experiments there [3, 7, 8]. MISS is a four storey steel frame, provided with movable masses on each storey and variable interstorey distances, which allows for different stiffnesses, mass profiles and eccentricities. This mock-up, weighting to 330 kN, was supported by six "further optimized" soft 125 mm diameter HDRBs (shear modulus G = 0.4

MPa) with an attachment system formed by a combination of central dowel and bolts (CDB) [1]. As far as tests at ARI are concerned, the superstructure (weighting 1,600 kN) was supported by four 250 mm diameter "further optimized" HDRBs with medium hardness rubber (G = 0.8 MPa) and CDB attachment system [1].

The considered actual buildings were one of the five TELECOM Italia buildings at Ancona (Fig. 2a) and the twin isolated and conventionally founded apartment houses at Squillace (Fig. 3a), where HDRBs have been installed [7, 8]. All the aforesaid buildings had been subjected to on-site tests by ISMES, on behalf of ENEL and ENEA, using a mechanical vibrator on the roof in various directions; in addition, the TELECOM Italia building at Ancona had been subjected to pull-back tests using collapsible devices provided with explosive bolts to release the displaced building [3, 7, 8]. For the Ancona building, the first tests allowed for the characterization of the superstructure, while the second - which were performed by gradually increasing the initial displacement to 110 mm (75% of the design value) - allowed for the evaluation of rigid body modes, thus also strongly contributing to the qualification of the SI system. For the Squillace buildings, which have smaller sizes, the SI effects were also sufficiently well detected in spite of relatively low excitation level.

For all above-mentioned mock-ups and buildings a large number of data was recorded in various locations at the different floors, axial positions and directions: these data were also very useful for the optimization of the seismic monitoring systems, which were installed by ENEL at both Ancona and Squillace.

EXPERIMENTAL TESTS ON THE STRUCTURE MOCK-UPS

Similar to previous mock-up tests [3, 7, 8], MISS was tested by appyling one-directional (1D), 2D and 3D simultaneous excitations corresponding to real earthquakes for various soil conditions and excitation levels. In addition, synthetic earthquakes, consistent with EuroCode-8 (EC8), were also applied. Among the results, it is worthwhile noting that [9]:
- quite large shear deformations were measured without any problem (up to 286% shear strain under the 3D simultaneous excitation corresponding to the Calitri record of the 1980 Campano-Lucano earthquake);
- the beneficial effects of SI were always very evident (with respect to the fixed-base structure), in spite of the very low isolation ratio (1.75), even when the shake table acceleration was amplified by a factor 100% at the MISS base under the aforesaid Calitri excitation (in general, however, deamplification of the input acceleration was measured on MISS).

The rigid superstructure mock-up was subjected to five pull-back tests at ARI; in these tests, the initial displacement was gradually increased up to the maximum value which was compatible with the used jack, namely 130% shear strain.

NUMERICAL MODELLING OF ISOLATORS

ENEL and ENEA analysed the results of all the above-mentioned tests, using the ABAQUS computer code, where implemented had been simplified models of the isolators and 3D finite-element models (FEMs) of the superstructures.

With regard to isolator modelling, it is noted that the FEMs described in ref. [1] are unnecessarily too complicated as to be applicable in the analysis of isolated structures. Thus, to this aim, the definition of simplified numerical models of the HDRBs, again based on the results of single HDRB tests, is necessary [7, 8]. Such models, however, shall be capable of

accounting for non-linear horizontal stiffness and the mostly hysteretic nature of damping. To this purpose the computer program ISOLAE of ENEA was first improved [7, 8], to enable the evaluation of the effects of the SI system on the excitation of the superstructure base and the subsequent FE calculation of the latter with the assumption of fixed base (in ISOLAE stiffness and viscous damping coefficient can be both assumed as dependent on lateral displacement).

Later, a new simplified model of the HDRBs which can be directly implemented in ABAQUS was jointly developed by ENEA and ENEL. This model (MEP, namely Multilinear Elastic-Plastic) consists of a non-linear spring combined with an elastic-plastic beam [7, 8]. By appropriately defining the physical parameters of the system (spring stiffness values, Young's modulus and yield point of the beam) it is possible to approximate the hysteresis cycle of a HDRB, including hardening and/or yielding and hysteretic damping. In fact, the non-linear spring allows for describing the dependence of horizontal stiffness on lateral deformation, while the beam permits to account for the hysteretic nature of damping, although not for its exact dependence on lateral deformation and for the viscous effects (the latter, however, may be included, if necessary, by adding a suitable viscous damper to the model). The advantage of MEP, with respect to ISOLAE, is that energy dissipation has been made independent of velocity.

NUMERICAL MODELLING OF ISOLATED STRUCTURES AND RESULTS OF THE ANALYSES

Detailed FE analysis of MISS was jointly performed by ENEA and ENEL with ABAQUS to design the mock-up itself and the test campaign; such a FEM was later used to analyse of the measured data (Fig. 1b). The analyses of the experimental results confirmed the adequacy of the numerical models used for both the isolators and MISS superstructure (good agreement was obtained between measurements and calculation for both natural frequencies and seismic response time-histories); however, they stressed the need for a careful selection of the damping value to be used, which shall be consistent with the maximum response displacement if the aim is, as usual, to correctly calculate such parameter (Fig. 1c, d): this may require some iterations of the dynamic calculations, if the experimental value is not known (see below).

As regards the TELECOM-Italia building, a 3D FEM of its superstructure (Fig. 2b), corresponding to the construction stage at the time of on-site tests, was developed by considerably refining the existing design model [7, 8]. It was validated and calibrated based on the results of the previously mentioned forced vibration tests. To this aim ENEA performed 3D parametric calculations where the building excitation conditions were exactly simulated and isolator stiffness and the damping values associated to the various modes of the isolated structure were defined based on best fit between computed and measured transfer functions (a linear spring was used to simulate the HDRBs, due to their very small deformation). The agreement between calculations and measurements was excellent [7, 8]. As expected for such small displacements, rather small damping ratios (2.8%) were found for the rigid body motions (modes 1 to 3), against the value 1.7% for modes 4 to 6, which are the first deformation modes of the superstructure.

The calculations concerning pull-back tests of the Ancona building were performed using a MEP model that was based on the results of single bearing tests performed at the building response frequency (0.8 Hz) in the lateral displacement range which had characterized the tests. The agreement between calculations and measurements was fully satisfactory, which confirmed the adequacy of the MEP model for seismic calculations of the building [7, 8]. It is

noted that the results previously obtained by means of ISOLAE runs were even better: the reasons are that the elastic-plastic beam of MEP model was calibrated on the data measured for the single HDRB at an average displacement (that of the pull-back test) and that viscous damping was fully neglected. In the above-mentioned previous calculations, however, the superstructure had been approximated by a rigid mass; furthermore, the model adopted in ISOLAE for energy dissipation (which remains proportional to the velocity) had been found to be not fully adequate for seismic excitation conditions.

Similar analysis was also performed by ENEL to validate and calibrate FEMs of both base isolated and conventionally founded houses at Squillace, again corresponding to the construction stages at the time of on-site tests (Fig. 3b). The agreement between calculations and measurements was again excellent [7, 8].

The final recent step of the analysis was, for both Ancona and Squillace buildings, the evaluation of earthquake effects in the case of both presence and absence of the SI system, and in the first case, with both the actually installed and the optimized HDRBs. Multidirectional excitations corresponding to the previously mentioned actual and synthetic earthquakes, were applied to FEMs of the completed Squillace buildings. For the Ancona building, only 1D excitations were applied in its longitudinal direction (so as to excite the first response frequency), because the FEM is much heavier and requires very long calculation time. MEP models of the isolators were initially based on the test results measured at 100% shear strain. Since calculations were elastic, some of them were performed with a Young's modulus decreased by 20% to simulate ductility. At least one iteration was necessary to evaluate the correct damping value characterizing the MEP model (see above).

The benefits of SI were found very large; in addition, also those related to the optimization of the HDRBs appear evident (Tables 1-3). For instance, in the case of a synthetic earthquake corresponding to EC8 for medium soil, the acceleration at the roof of the TELECOM-Italia building would be 13% of that corresponding to fixed base with the presently installed isolators and only 7% in the case of the optimized HDRBs; accordingly, the relative displacements between roof and superstructure base would be 56% and 37% of the fixed base values. The use of optimized HDRBs would also reduce to 50% the roof accelerations and to 60% the relative displacements under the Calitri record of the 1980 Campano Lucano earthquake (relatively soft soil), which would be less severe than the previous excitation. With regard to the isolator lateral deformations, only for the aforesaid EC8 excitation the design value of 140 mm would be slightly exceeded (although less for the optimized isolators than for those installed at present). Similar effects were found for the Squillace buildings (Figs. 3c, d).

CONCLUSIONS

The results of experimental tests and numerical analyses of isolated structure mock-ups and actual buildings demonstrated the large benefits of seismic isolation systems, in particular those formed by the optimized HDRBs developed in project [2], on the design of buildings. This result is consistent with the observations of the behaviour of isolated buildings during the 1994 Northridge and 1995 Great Hanshin-Awaji earthquakes. The adequacy of the developed simplified numerical models of the isolators and FEMs of the superstructures was also demonstrated.

REFERENCES

1. Forni, M., A. Martelli, B. Spadoni, G. Venturi, A. Dusi, F. Bettinali, G. Bonacina, G. Pucci, A. Marioni, C. Mazzieri & F. Cesari 1997. Development and validation of FEMs for the design and qualification of HDRBs for seismic isolation.
Proc. 14th SMiRT Conf. Lyon, France.

2. Enel, Alga, Dywidag, Enea, Mrpra, Shw & Stin 1993. Optimization of design and performance of high damping rubber bearings for seismic and vibration isolation.
EC Contract BRE2-CT93-0524, Project BE7010, Bruxelles, Belgium.

3. Forni, M., A. Martelli, B. Spadoni, G. Vernoni, F. Bettinali, A. Marioni, G. Bonacina, C. Mazzieri & F. Vestroni 1993. Most recent experimental and numerical studies performed in Italy on seismic isolation.
Proc. 12th SMiRT Conf. Vol. K2: 225-236. Amsterdam: North Holland.

4. Forni, M., A. Martelli, A. Dusi & G. Castellano 1995. F.E. models of steel-laminated rubber bearings for seismic isolation of nuclear facilities.
Proc. 13th SMiRT Conf. Vol. III: 603-614. Porto Alegre, Brasil.

5. Martelli, A., M. Forni, B. Spadoni, A. Marioni, C. Mazzieri, F. Bettinali, G. Bonacina, G. Pucci, F. Cesari & E. Sobrero 1995. Progress in applications and experimental studies for isolated structures in Italy.
Proc. Int. Post-SMiRT Conf. Seminar on Seismic Isolation, Passive Energy Dissipation and Active Control of Vibrations Structures. Santiago, Chile.

6. Forni, M., A. Martelli, F. Bettinali & A. Dusi 1995. Finite element models of rubber bearings and guidelines development for isolated nuclear facilities in Italy.
Proc. Int. Post-SMiRT Conf. Seminar on Seismic Isolation, Passive Energy Dissipation and Active Control of Vibrations Structures. Santiago, Chile.

7. Martelli, A., M. Forni, M. Indirli, B. Spadoni, F. Bettinali, A. Dusi, A. Marioni, G. Bonacina, G. Pucci & C. Mazzieri 1996. Italian studies for the optmization of seismic isolation systems for civil and industrial structures.
Proc. 11WCEE. Acapulco, Mexico.

8. Martelli, A., M. Forni, F. Bettinali, A. Dusi, G. Bonacina & A. Marioni 1996. Current activities on the use of high damping rubber isolation bearings in Italy.
Proc. Fourth Worl Congress on Joint Sealing & Bearings Systems for Concrete Structures. Sacramento, California, USA.

9. Bonacina, G., G. Pucci, A. Marioni, H. Baumann, W. Krause, F. Bettinali, A. Dusi, M. Forni, A. Martelli, M. Indirli, A. Muhr, C. Mazzieri, J. Eibl & K.H. Hehn. Tests and analysis of optimized high damping rubber bearings, base isolated structure mock-ups and actual isolated buildings.
Proc. Int. Post-SMiRT Conf. Seminar on Seismic Isolation, Passive Energy Dissipation and Active Control of Structures. Taormina, Italy.

Fig. 1a. MISS mock-up on the ISMES shake table in the fixed-base configuration with 16 masses (240 kN)

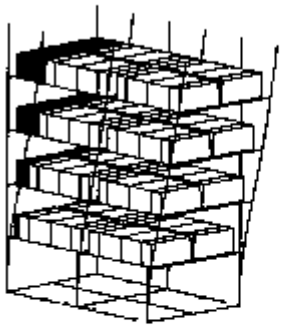

Fig. 1b. FEM of the MISS mock-up with 16 masses (240 kN); first bending mode (F_1=1.49 Hz; experim. = 1.5 Hz; α=1.75)

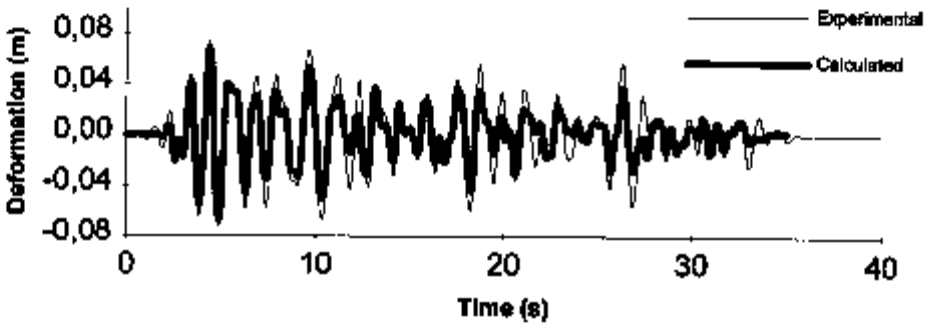

Fig. 1c. Bearing deformation measured and calculated for the isolated MISS mock-up with 20 masses (290kN) in the case of the application of a synthetic earthquake (0.3 g max acceleration peak)

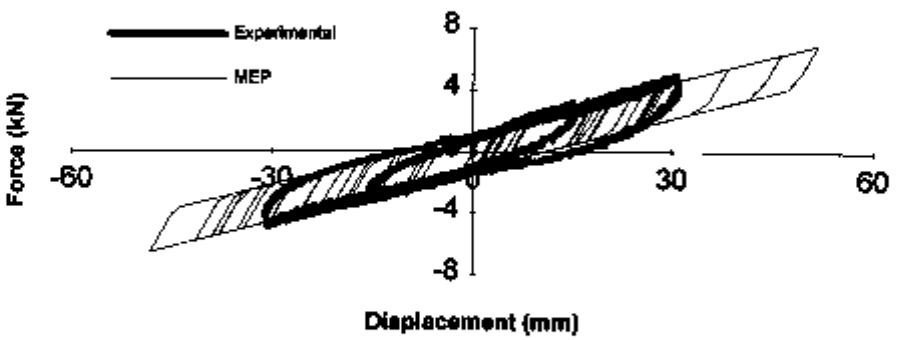

Fig. 1d. Comparison between the hysteresis loops as calculated by the MEP model (synthetic earthquake 0.2 g peak) for isolated MISS mock-up with 20 masses and that obtained by static test on single isolator

Fig. 2a. TELECOM Italia building at Ancona during construction (1990) and in-situ tests

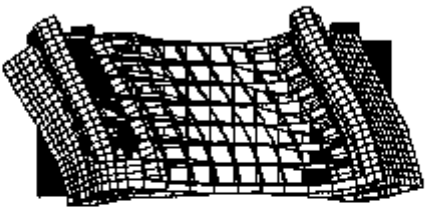

Fig. 2b. FEM of the TELECOM Italia building (first bending mode, fourth global mode, F_1=4.8 Hz)

Tab. 1: Relative maximum displacement values between roof and superstructure base. Summary of all analysed cases.Earthquake in horizontal longitudinal direction [cm].
**: Standard Young's Modulus; **: Decreased (- 20 %) Young's Modulus*

EARTHQUAKES	CALITRI 1980 *	CALITRI 1980 **	TOLMEZZO 1976 *	TOLMEZZO 1976 **	EC8 *	EC8 **
Fixed Base	-	1.58	-	2.17	1.79	2.36
Actual HDRBs	0.89	-	-	-	1.00	-
Optimized HDRBs	0.55	-	0.30	-	0.67	-

Tab. 2: Displacements of bearings. Summary of all analysed cases. Earthquake in horizontal longitudinal direction [cm]. Telecom Italia Building at Ancona: Design Displacement 14 cm.
**: Standard Young's Modulus; **: Decreased (- 20 %) Young's Modulus*

EARTHQUAKES	CALITRI*	TOLMEZZO*	EC8*
Actual HDRBs	14.27	-	16.72
Otimized HDRBs	11.25	5.27	15.88

Tab. 3: Relative maximum acceleration values between roof and superstructure base. Summary of all analysed cases. Earthquake in horizontal longitudinal direction [cm/s^2].
**: Standard Young's Modulus; **: Decreased (- 20 %) Young's Modulus*

EARTHQUAKES	CALITRI *	CALITRI **	TOLMEZZO *	TOLMEZZO **	EC8 *	EC8 **
Fixed Base	-	627.7	-	102.4	846.6	1069.0
Actual HDRBs	97.86	-	-	-	110.5	-
Optimized HDRBs	49.12	-	46.35	-	60.34	-

Fig. 3a. Isolated apartment house at Squillace during construction and in-situ tests (1991)

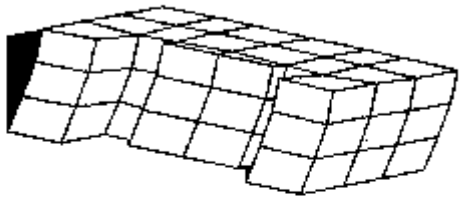

Fig. 3b. FEM of the isolated Squillace apartment house (first bending mode, fourth global mode, F_1=5.3 Hz))

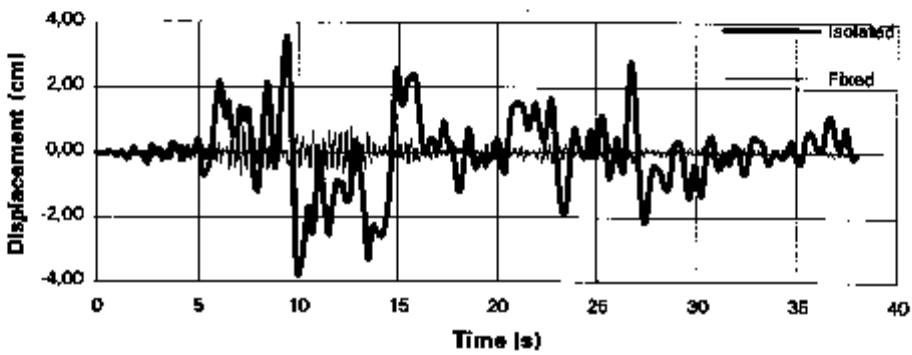

Fig. 3c. Absolute displacement as calculated at the roof of the Squillace isolated building compared to that obtained in the case of fixed-base in the case of application of the 3D 1980 Calitri record

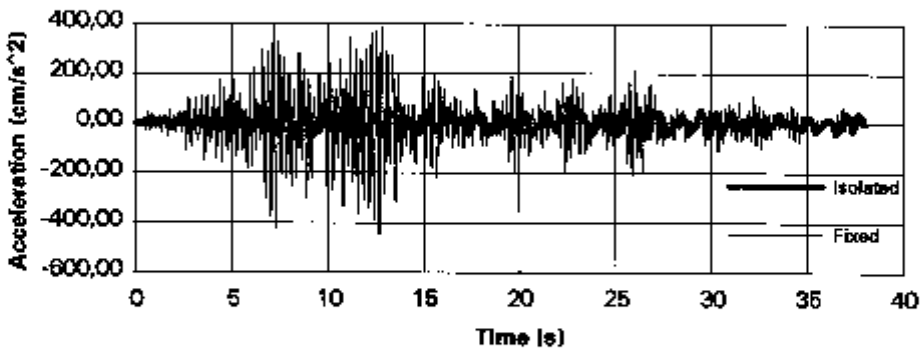

Fig. 3d. Acceleration as calculated at the roof of the Squillace isolated building compared to that obtained in the case of fixed-base in the case of application of the 3D 1980 Calitri record

Transactions of the 14th International Conference on Structural Mechanics in Reactor Technology (SMiRT 14), Lyon, France, August 17-22, 1997 K11/1

Optimization of structural layout of 3-D low-frequency seismic isolation system of reactor building

Bellayev V.S.[1], Vinogradov V.V.[1], Petrenko V.A.[1], Privalov S.Y.[1], Kostarev V.V.[2]
(1) Scientific Research Center, Russia
(2) CKTI Vibroseism, Russia

ABSTRACT: The problems of choosing the optimal layout of the seismic isolation devices for 3-D low-frequency seismic isolation system of a reactor building are discussed in the paper. The influence of the base slab deformability on the response values of the seismic isolators has been investigated. The results of numerical analysis illustrate distribution of the seismic isolators responses for the soils with various stiffness degree.

INTRODUCTION

Application of the 3-D seismic isolation of a reactor building introduces a series of special features into the structural layout of the building. Consideration is being given to the main of them: presence (in addition to the nuclear reactor building base slab which transmit load from the seismic isolators to the building) of the additional base slab, on which the seismic isolation system is located. Deformability due to the this plate dimensions would have a profound effect on the seismic isolators response in accordance to their layout and stiffness degree of the foundation soil. Seismic isolation system realization as an element of the building foundation involves determination of the possible limitations.

SET OF LIMITATIONS, ASSOCIATED WITH OPERATION CONDITIONS OF THE SEISMIC ISOLATION SYSTEM

Procedure of choosing the rational layout of the seismic isolators under a nuclear reactor building which is based on strengths investigation and base slabs deformability has a series of limitations.

The main limitations can be formulated as follows:

- limitations on the maximum stresses $\delta(x,t)$, acting in the base slabs sections under the static and dynamic loads

$$\max_i \delta^1(x,t) < [\delta], \qquad (1)$$

i=1 - for the building base slab;

i=2 - for the base slab of the structure as a whole

$[\delta]$ - allowable stresses for the reinforced concrete of the corresponding grade:

- limitations on the maximum conceivable inclinations of the embedded pieces in the seismic isolation bearings at the base slabs deformations under all loading conditions:

$$\max_i |H_i - H_i^0| < \delta, \; i \; (1,N), \qquad (2)$$

where H_i^0 - eccentric distance of embedded pieces of the ith support, which are located on the base slabs;

H_i - distance between the points which are located on the embedded pieces circuits of the ith support;

N - number of supports in the seismic isolation system;

δ - permissible value of nonhorizontality of the embedded elements surfaces;

- limitation on the overall dimensions of the seismic isolation bearings under the condition of sufficient load-carrying capacity:

$$\min r > \max (\min r_{imaint}, \min r_{erect}), \; i \; (1,1) \qquad (3)$$

$$NxQ > G,$$

where r - minimum distance between the seismic isolation bearings (or supports and lateral walls of the base slab);

r_{imaint} - minimum distance between the supports, needed for servicing and repairing the i-type supports, prescribed according to the specifications;

r_{erect} - minimum distance between the supports,

specified in accordance with the technological requirements on the system installation;

l - number of the support types used in the system;

Q - load-carrying capacity of one device;

G - maximum total weight of the protected object;

N - total number of the seismic isolation bearings;

- limitation on the value of the spread in forces in the supports ΔP relatively the average P level:

$$\Delta P \longrightarrow \min, \text{ where } \Delta P = P_i - P, \; i \; (1,N) \qquad (4)$$

P_i - force in the ith support.

Introducing the last limitation is related to the fact that when the reactor building is under construction there are used technological (erection) supports, which after the construction ending are replaced by the seismic isolators. Removal of the erection supports is possible only in the event that the building weight load would be removed from them. In the seismic isolation system in question the release of the erection supports is produced by filling all of the pneumoshock-absorbers and does not involve any additional devices.

DESIGN CONDITIONS

For the seismic isolation system loads on the nuclear reactor building and the base slab there had been taken the forces, arising in the supports (seismic isolators or erection supports) under various conditions of system operation on the object construction and operation steps.

Calculation of the loads acting on the reactor building base slab in the layout positions of the seismic isolation system supports was carried out under the following conditions:

1. Vertical loads act on the embedded pieces compression, horizontal ones - on their shear, in this condition the design loads application area has circular form which is symmetrical relatively the embedded piece centre.

2. Loads to the base slab are applied in accordance with the

seismic isolation bearings layout.

3. The following design loading modes were considered: construction mode, pneumoshock-absorbers filling mode, operation mode.

4. For the construction mode there was specified the value of the centre of mass displacement of the object under construction at various total mass values. Under this condition there was assumed, that on the steps which precede the reactor building construction completion, possible centre of mass displacement will be less, than on the initial steps.

5. For the pneumoshock-absorbers filling mode there was assumed that the pressure variations in all the devices are simultaneous, in this condition until the forces in the support does not exceed the erection forces, stiffness of the element which simulates a support, corresponds the strut stiffness.

6. Under operation conditions there was assumed, that 0,9 of the total reactor building mass is perceived by devices with monotonous force characteristic, and 0,1 of the total mass - by devices which form a step characteristic. Calculations were carried out for the case of the total reactor building mass.

METHOD OF ANALYSIS

To design a reactor building seismic isolation system under the static loads action there was used a finite-element model of the reactor building and the lower base slab with the corresponding boundary conditions. As a basic finite element there had been taken a triangular element of a thin plate. This element has 18 degrees of freedom.

As a boundary element in the shock-absorber model we use a single-degree-of-freedom element.

Reactor building foundation was simulated with the use of single-degree-of-freedom elements of simple stiffness, which were located in each node of the finite-element model of the lower base slab. As the soil pressure was considered as applied in the model nodes, for each node there was

determined the soil pressure application area as a part of the triangular elements area, which are contiguous to a node under consideration with this node centre of gravity.

Finite-element model of the seismic isolated reactor building is performed based on the building construction representation as a spatial system of triangular plate elements and boundary elements in the isolator installation places. The total number of node connections is 244; the total number of triangular elements is 474.

Elements thicknesses were specified in accordance with the thickness of walls and floors in a real structure. Since a building construction has two-plane symmetry, in the calculation there was used one quarter of the construction with corresponding boundary conditions on the planes of symmetry which exclude rotation about the OX and OY axes for the planes 1 and 2 respectively and displacements in the OY and OX direction for the planes 1 and 2 respectively. In the calculation there were simulated both the lower and the upper base slabs, as well as the building lower part up to 10,5 m elevation. Mass of the structures and components, which were above this level was acconted for as an external distributed load on the cylindrical and radial walls.

Precomputations have indicated, that minimization of ΔP value ensures the best conditions of load redistribution on the base slabs.

As an example, in the Table 1 there are presented the results of solving the problem of seismic isolators layout for a reactor building, located on the "soft" foundation soil.

Base slabs thickness was:

1.5 m - for the building base slab;

3.0 m - for the structure base slab.

CALCULATIONS RESULTS

For the chosen layout of the seismic isolation bearings (Tab. 1) with the fixed structure base slab thickness (3m)

investigations had been performed to evaluate the foundation stiffening effect on the force distribution of in the supports. In the calculations the soil stress-strain modulus E altered within the range from 16 MPa ("soft" soil) up to 2500 MPa ("hard" soil). Separately the case of undeformable foundation had been considered.

Table 1

Radius of supports installation, m	Number of supports	P, t	max ΔP, t
22.7	27	853.75	0.05
20.3	35	851.0	2.5
15.4	4	843.2	-
12.0	4	840.0	-
8.9	12	870.3	-
5.5	6	890.2	-
0.0	1	883.0	-
For seismic isolation system as a whole	89	856.6	33.6

As a parameter for comparison of the alternate calculation modes we had chosen the deviation ΔP of the average force P_{av} from the force which corresponds to the pneumoshock-absorbers filling pressure (equal for all of them) P_{fill}, for each radia of support installation. For the corresponding radius of support installation (see Tab.1) the average force P_{av} was determined according to the formula:

$$P_{av} = (\sum_{1} P_i) / N_1 \qquad (5)$$

where P_i - the forces in the ith supports;

N_1 - number of supports on the corresponding radius of the installation.

Analysis of calculation results P_{av} has shown, that when the stiffness of the foundation soil increases the deviations of forces P_i from the average value have a reduction

tendency.

Fig. 1 presents the calculations results ΔP for six types of soils. Analysis of the calculation results has shown that: - for the chosen seismic isolation bearings layout the use of the structure base slab with 3m thickness is allowable for the soils with stress-strain modulus E within the limits 50MPa - 200 MPa; - supports, located on the "external" radia of the installation (R>15.4m), practically for any ground conditions turn out to be "underloaded" ($P_{av} < P_{fill}$); - supports, located on the "internal" radia of the installation (R <15.4m), more commonly turn out to be "overloaded" ($P_{av} > P_{fill}$); - for too "hard" soils (E>200Mna) it is required to change the filling pressure of the pneumoshock-absorbers, located on the "internal" radia of the placement, or to change the layout adding one support more; - for too "soft" soils (E < 50Mna) it is required to increase the structure base slab thickness.

CONCLUSION

The results received testify that the absence of requirement on the geometry invariability of the base slab, (i.e. assumption of its deformability) does not cause special difficulties when the system is used as a vertical seismic isolation of pneumatic elements taking into account the limitations, connected with the object operation under normal conditions.

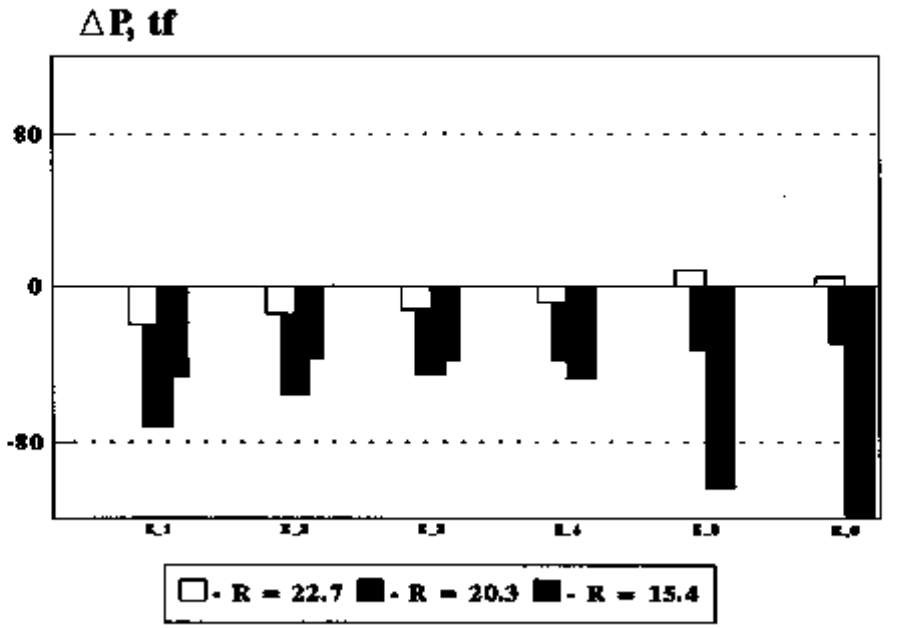

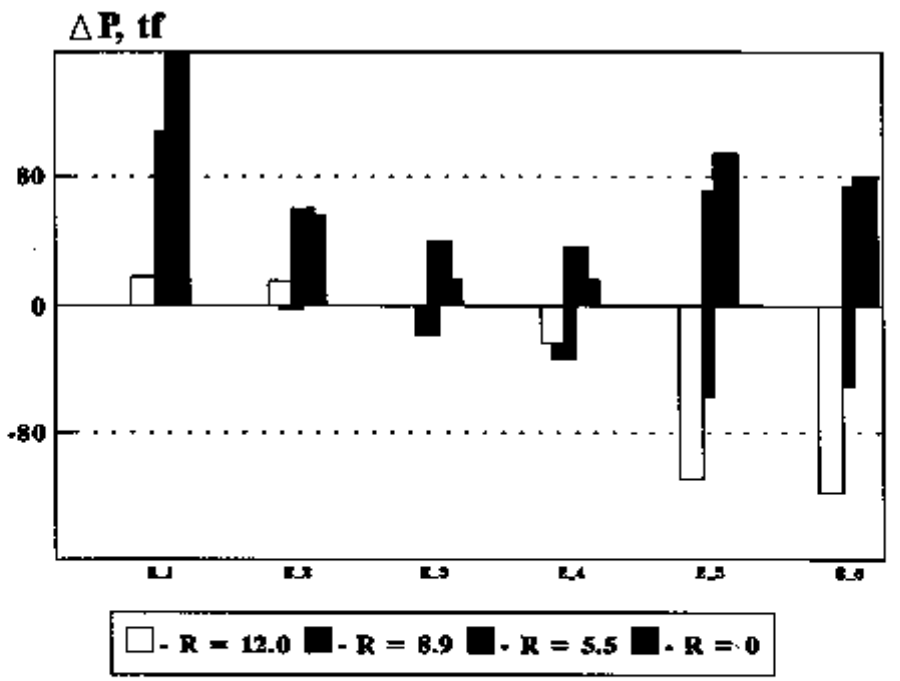

Fig.1 Dependence of ΔP deviation from the foundation soil stiffness